



Recent Development of Thermoelectric Polymers and Composites

Hongyan Yao, Zeng Fan, Hanlin Cheng, Xin Guan, Chen Wang, Kuan Sun,* and Jianyong Ouyang*

Thermoelectric materials can be used as the active materials in thermoelectric generators and as Peltier coolers for direct energy conversion between heat and electricity. Apart from inorganic thermoelectric materials, thermoelectric polymers have been receiving great attention due to their unique advantages including low cost, high mechanical flexibility, light weight, low or no toxicity, and intrinsically low thermal conductivity. The power factor of thermoelectric polymers has been continuously rising, and the highest ZT value is more than 0.25 at room temperature. The power factor can be further improved by forming composites with nanomaterials. This article provides a review of recent developments on thermoelectric polymers and polymer composites. It focuses on the relationship between thermoelectric properties and the materials structure, including chemical structure, microstructure, dopants, and doping levels. Their thermoelectric properties can be further improved to be comparable to inorganic counterparts in the near future.

is called power factor (PF). TE materials can be classified into p-type and n-type materials in terms of the charge carriers. Holes and electrons are the major charge carriers for the former and the latter, respectively. Efficient inorganic TE materials are semiconductors or semimetals. They usually have high Seebeck coefficient and moderate electrical conductivity. Although many organic conductors and semiconductors also exhibit thermoelectric behavior, in early days these materials have no practical significance due to their low ZT values.^[5,6] However, great progress was made on organic thermoelectric materials recently. High thermoelectric properties close to inorganic TE materials were observed on some intrinsically conductive polymers. Polymers are promising to be the next generation TE materials arising

from their unique advantages including low cost, high mechanical flexibility, light weight, low or no toxicity, and intrinsically low thermal conductivity.^[5,7,8]

The ZT value depends on the PF value and the thermal conductivity. The thermal conductivity of polymers is usually less than $1 \text{ W m}^{-1} \text{ K}^{-1}$ and difficult to further decrease. In contrast, the PF value of the conductive polymers can be significantly enhanced by several orders of magnitude. Therefore the PF value is usually used to evaluate the TE properties of polymers. The PF depends on both the Seebeck coefficient and the electrical conductivity. The electrical conductivity of a material is generally expressed by the equation, $\sigma = nq\mu$, where q is the elementary charge, n is the charge carrier concentration, and μ is the charge carrier mobility. As PF is proportional to the electrical conductivity, almost all the TE polymers are conductive polymers. The charge carrier concentration of conductive polymers is affected by the doping level, and the charge carrier mobility is related to the chemical structure and morphology.^[6] S represents the entropy of a carrier with unit charge, which is governed by the following equation in a simplified system of charge carriers without strong interactions, $qS = k_B \ln[(1 - \rho)/\rho]$, where ρ is the charge density.^[5] Thus the Seebeck coefficient and electrical conductivity are interdependent. Generally, lowering the charge carrier concentration can increase the Seebeck coefficient while decrease the electrical conductivity. Hence, there is an optimal doping level for high PF.

Apart from approaches to improve the TE properties of neat polymers, another popular approach is to form composites of

1. Introduction

Thermoelectric (TE) materials can exhibit electrical voltage when there is a temperature gradient at two ends. They can be used as the active materials of TE generators and Peltier coolers that can directly convert energy between heat and electricity. Because there is no mechanically moving parts in these TE devices, they are quiet and compact. The energy conversion efficiency of a TE generator or Peltier cooler depends on the figure of merit (ZT) of the TE materials, $ZT = S^2 \sigma T / \kappa$, where S is Seebeck coefficient or thermopower, σ is electrical conductivity, κ is thermal conductivity, and T is absolute temperature.^[1-4] $S^2 \sigma$

Dr. H. Yao, Dr. Z. Fan, Dr. H. Cheng, X. Guan, Prof. J. Ouyang
Department of Materials Science and Engineering
National University of Singapore

Singapore 117574, Singapore
E-mail: mseoj@nus.edu.sg

C. Wang, Prof. K. Sun
Key Laboratory of Low-Grade Energy Utilization Technologies and Systems
Ministry of Education
School of Power Engineering
Chongqing University
Chongqing 400044, China
E-mail: kuan.sun@cqu.edu.cn

The ORCID identification number(s) for the author(s) of this article can be found under <https://doi.org/10.1002/marc.201700727>.

DOI: 10.1002/marc.201700727

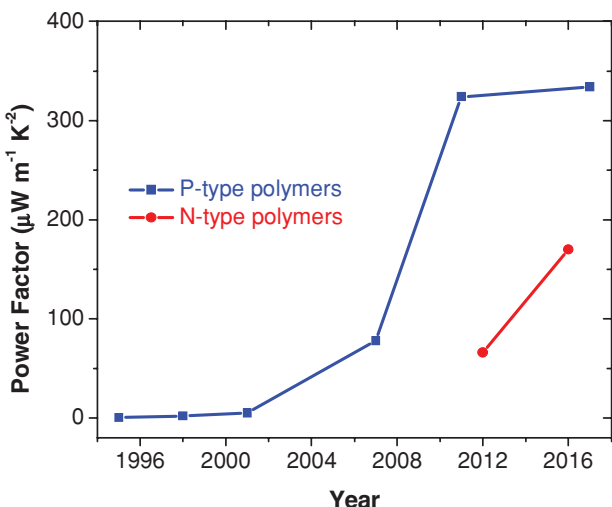


Figure 1. Milestones of the power factors of p-type and n-type TE polymers.

polymers with nanomaterials. The nanofillers can increase the electrical conductivity and/or the Seebeck coefficient of the polymer matrix, but they usually do not increase the thermal conductivity remarkably when their loading is not too high. Therefore, TE polymer composites can have high mechanical flexibility and low thermal conductivity similar to the thermoelectric polymers.

Great progress has been made on p-type and n-type TE polymers as well as polymer composites (Figure 1). This article provides a review on the recent development of TE polymers and composites. We believe that the TE properties of polymers can be comparable to their inorganic counterparts in near future. This will enable the development of flexible and portable TE systems.

2. p-Type TE Polymers

Intrinsically conductive polymers usually have conjugated backbone in either oxidized or reduced state. The charge carriers are holes when the polymers are in the oxidized state. The representative p-type TE polymers include poly(3,4-ethylenedioxythiophene) (PEDOT), polythiophene derivatives, polyacetylene (PA), polyaniline (PANI), polypyrrole (PPy), polycarbazole, and polyphenylenevinylene (PPV) derivatives.

2.1. PEDOT:PSS

The PEDOT family is the most popular TE polymers because of their high TE properties. In particular, PEDOT:poly(styrenesulfonate) (PEDOT:PSS, chemical structure shown in Figure 2a) has received the greatest attention because it can be processed by solution processing techniques when in its doped state. The TE properties of some typical PEDOT:PSS are listed in Table 1.

PEDOT:PSS can be dispersed in water, and its aqueous solutions are commercially available. But as-prepared PEDOT:PSS film from its aqueous solution has low TE properties with



Kuan Sun is an assistant professor at the School of Power Engineering, Chongqing University, China. He received his B.Apl.Sci. (Hon.) and Ph.D. degree from the National University of Singapore (NUS), and postdoc trainings at the University of Melbourne and NUS. He was also a visiting scholar at Karlsruhe Institute of Technology and the Max Planck Institute for Polymer Research. His research focuses on printable solar cells, transparent electrodes, thin-film thermoelectric materials, as well as novel functional materials and devices.



Jianyong Ouyang received his Ph.D., master's, and bachelor's degrees from the Institute for Molecular Science in Japan, the Institute of Chemistry of the Chinese Academy of Science, and Tsinghua University in Beijing, respectively. He worked as an assistant professor at the Japanese Advanced Institute of Science and Technology and as a postdoctoral researcher at the University of California, Los Angeles (UCLA), before joining the National University of Singapore as an assistant professor in 2006. He was promoted to associate professor in 2012. His research interests include flexible electronics and energy materials and devices.

the electrical conductivity $<1 \text{ S cm}^{-1}$, Seebeck coefficient of $\approx 15 \text{ } \mu\text{V K}^{-1}$ and PF of $\approx 0.008 \text{ } \mu\text{W m}^{-1} \text{ K}^{-2}$.^[9–18] Such poor properties are related to the excess PSS that is needed to stabilize PEDOT in water.^[10] Removing the excess PSS can significantly enhance the TE properties particularly the electrical conductivity of PEDOT:PSS. A couple of methods were developed to enhance the conductivity of PEDOT:PSS.^[19–45] Moreover, the Seebeck coefficient can be improved by dedoping, since as-prepared PEDOT:PSS with a doping level of around 30% has a low Seebeck coefficient.^[9]

2.1.1. Secondary Doping of PEDOT:PSS

Secondary doping is usually carried out by adding a chemical into PEDOT:PSS aqueous solution or treating a PEDOT:PSS film with solvent, vapor, or solution. It can enhance the conductivity of PEDOT:PSS since it modifies the PEDOT:PSS composition and film morphology without changing the doping level. The enhancement of the electrical conductivity of PEDOT:PSS

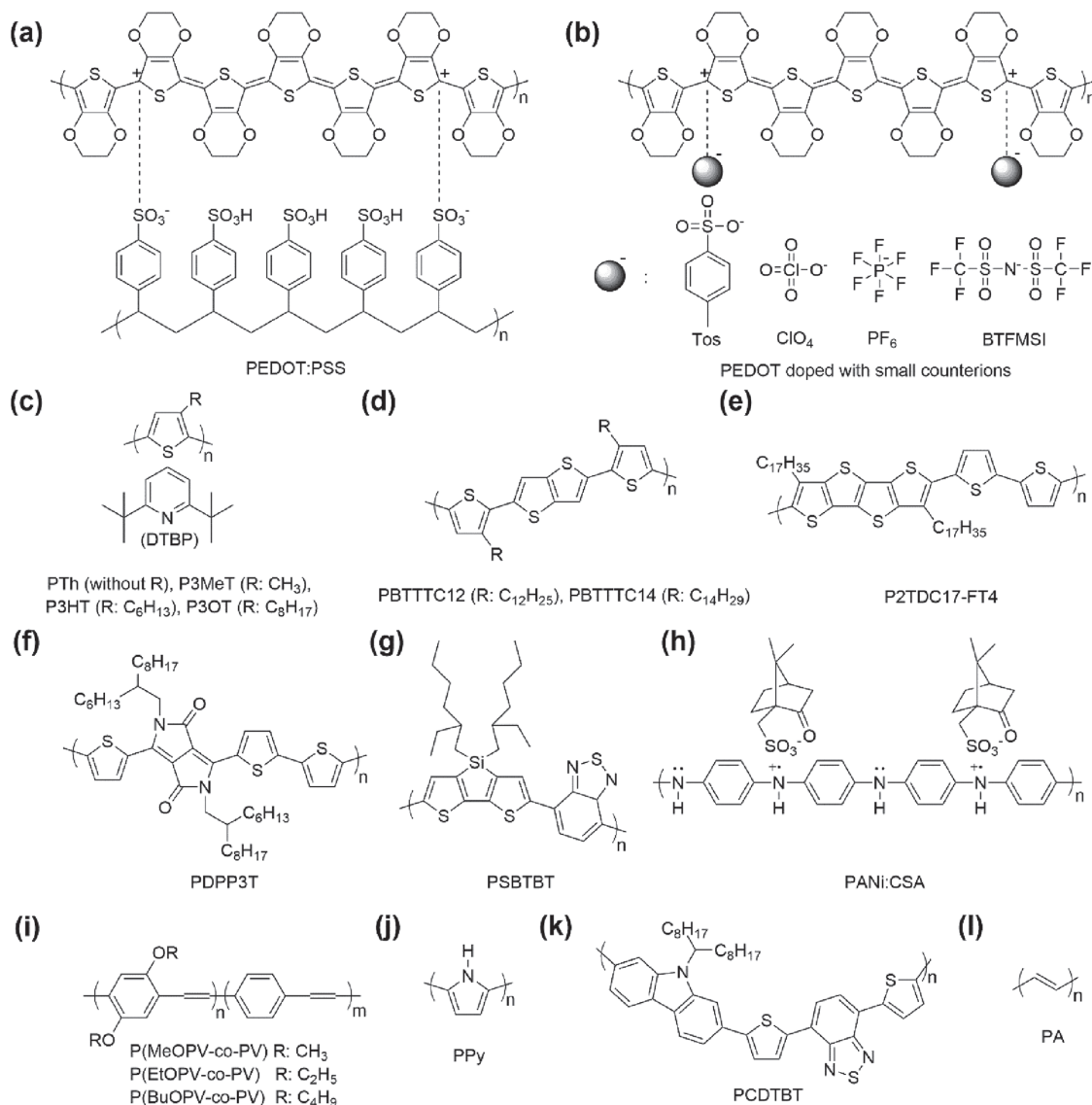


Figure 2. Chemical structures of representative polymer TE materials: a) PEDOT:PSS, b) PEDOT doped with small counterions, c) PTh, P3MeT, P3HT, and P3OT, d) PBTTTC12 and PBTTTC14, e) P2TDC17-FT4, f) PDPP3T, g) PSBTBT, h) PANi:CSA, i) PPV derivatives, j) PPy, k) PCDTBT, and l) PA.

Table 1. Summary of the TE properties of various treatments of PEDOT:PSS.

Treatment	S [μV K ⁻¹]	Σ [S cm ⁻¹]	PF [μW m ⁻¹ K ⁻²]	κ [W m ⁻¹ K ⁻¹]	ZT at r.t.	Ref.
Addition of DMSO and PEO	38.4 ± 7.1	1061 ± 16	157.35	—	—	[29]
Posttreatment with FA	20.6	1900	80.6	—	—	[37]
Posttreatment with DMF solution of ZnCl ₂	26.1	1400	98.2	—	—	[43]
Electrochemical dedoping	≈100	≈20	23.5	—	0.041	[47]
Chemical dedoping with AF	436.3	0.036	0.69	0.32	1.1 × 10 ⁻³	[48]
Treated with EMIM-BF ₄ and DMSO	≈23	≈700	38.46	0.17	≈0.068	[49]
Treated with DMSO then DMSO and HZ	≈41	677	115.48	≈0.17	0.2	[50]
Treated with NaOH	≈15.8	≈800	≈19.6	—	—	[52]
Treated with HZ	67	578	112	0.366 ± 0.016	0.093	[53]
Treated with TSA and then HZ and DMSO	≈50	≈1300	318.4	0.3	0.31	[54]
Treated with H ₂ SO ₄ and then NaOH	39.2	2170	334	—	—	[56]

by secondary doping has been reviewed.^[28] The secondary doping can enhance the PF of PEDOT:PSS as well.

The TE performance of PEDOT:PSS can be enhanced by adding a chemical compound such as dimethyl sulfoxide (DMSO), ethylene glycol (EG), or poly(ethylene oxide) (PEO) into its aqueous solution.^[19–29] For example, DMSO can enhance the electrical conductivity by up to three orders of magnitude while it has negligible effect on the Seebeck coefficient.^[19] Gong et al. found that the addition of both PEO and DMSO can enhance not only the electrical conductivity but also the Seebeck coefficient.^[29] They thus observed an optimal PF of $157.4 \mu\text{W m}^{-1} \text{K}^{-2}$ with the electrical conductivity of 1300 S cm^{-1} and Seebeck coefficient of $40 \mu\text{V K}^{-1}$.

The secondary doping can be done through posttreatment of PEDOT:PSS films as well.^[30–45] For instance, Chu et al. investigated the posttreatment of PEDOT:PSS films with organic solvents including methanol and formic acid.^[37] After treated with formic acid, the PEDOT:PSS films can exhibit a PF of $80.6 \mu\text{W m}^{-1} \text{K}^{-2}$ with the electrical conductivity of 1900 S cm^{-1} and Seebeck coefficient of $20.6 \mu\text{V K}^{-1}$. Using the Harman method, they estimated that the in-plane ZT value was 0.12 and the vertical ZT value was 0.32 at room temperature.

In addition to neat organic solvents, solutions were also used for the posttreatment. It has been reported that an organic solution of an inorganic salt can have a synergistic effects on improving the TE properties of PEDOT:PSS.^[43] For example, treating PEDOT:PSS films with a *N*, *N*-dimethylformamide (DMF) solution of ZnCl_2 can improve their electrical conductivity and Seebeck coefficient simultaneously. The treatment of PEDOT:PSS films with 1 M ZnCl_2 in DMF can enhance the electrical conductivity to more than 1400 S cm^{-1} and the Seebeck coefficient to $26.1 \mu\text{V K}^{-1}$. The optimal PF is $98.2 \mu\text{W m}^{-1} \text{K}^{-2}$. The polar solvents and cations are able to weaken the Coulombic interaction between PEDOT and PSS chains, leading to the partial PSS removal, conformational change of PEDOT chains and morphological change of PEDOT:PSS films.

2.1.2. Dedoping of PEDOT:PSS

The Seebeck coefficient of PEDOT:PSS can be enhanced by tuning its doping level, because the doping level can affect both the band structure and the density of states (DOS).^[6,46] As-prepared PEDOT:PSS usually has low Seebeck coefficient due to the high doping level. Dedoping can remarkably enhance the Seebeck coefficient. But there exists an optimal doping level, as dedoping lowers the electrical conductivity. Dedoping can be carried out chemically or electrochemically. Crispin et al. dedoped PEDOT:PSS electrochemically in a configuration of organic electrochemical transistor.^[47] A high gate voltage led to the dedoping of PEDOT:PSS, and it consequently increased the Seebeck coefficient while lowered the electrical conductivity (**Figure 3**). They observed an optimal PF of $23.5 \mu\text{W m}^{-1} \text{K}^{-2}$ with the electrical conductivity in the range of $0.3\text{--}300 \text{ S cm}^{-1}$ and a Seebeck coefficient of $20\text{--}400 \mu\text{V K}^{-1}$ when the doping level was lowered from 33% to 14.5%. The PEDOT:PSS films can also be dedoped by reducing agents like hydrazine (HZ), ammonium formate (AF), 1-ethyl-3-methylimidazolium tetrafluoroborate (EMIM-BF_4^-), sodium borohydride (NaBH_4), or

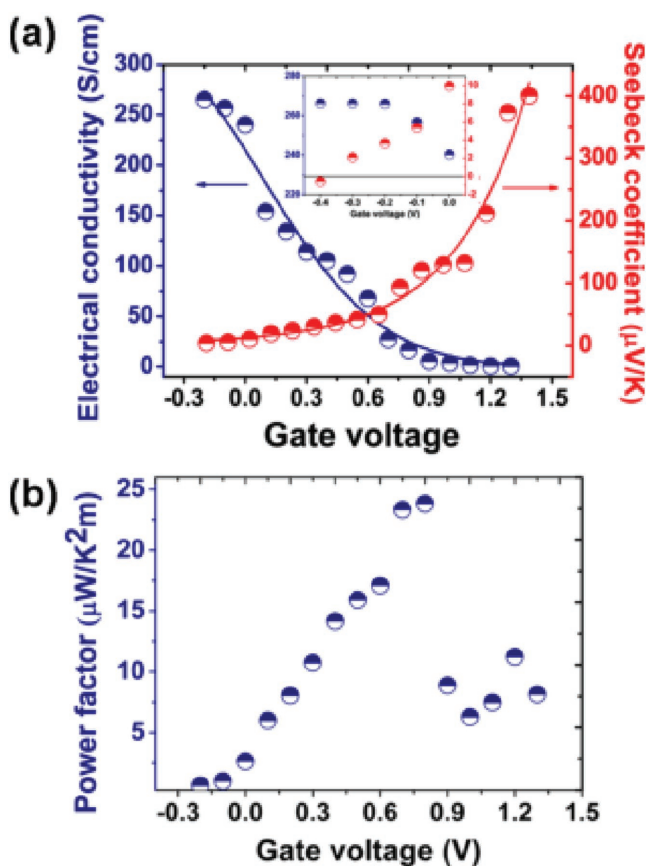


Figure 3. a) Electrical conductivity (blue symbols) and Seebeck coefficient (red symbols). b) PF of PEDOT:PSS as functions of gate voltage. Reproduced with permission.^[47] Copyright 2012, The American Chemical Society.

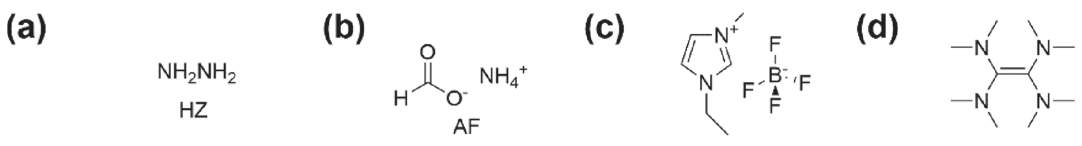
hydroiodic acid (HI), etc.^[16,48–51] The chemical structures of HZ, AF, and EMIM-BF_4^- are shown in **Figure 4a–c**.

In addition, a chemical reducing agent together with an organic solvent can be used for the purpose of conductivity enhancement and dedoping. For example, Luo et al. treated the PEDOT:PSS films using a mixture of DMSO and EMIM-BF_4^- that is both a reducing agent and an ionic liquid.^[49] The treatment changes the majority charge carriers from bipolarons to polarons. As a result, the Seebeck coefficient increases from ≈ 15.7 to $\approx 23 \mu\text{V K}^{-1}$, and electrical conductivity decreases from 900 to $\approx 700 \text{ S cm}^{-1}$. The optimal PF is $38.46 \mu\text{W m}^{-1} \text{K}^{-2}$.

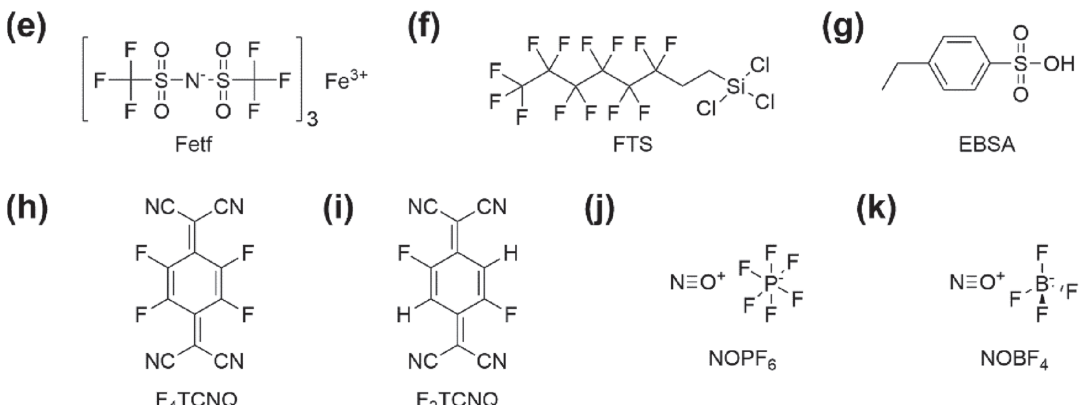
2.1.3. Sequential Treatments of PEDOT:PSS

As mentioned above, secondary doping can enhance mainly the electrical conductivity, while dedoping can increase the Seebeck coefficient but lower the electrical conductivity. Therefore, sequential treatments of secondary doping and dedoping may give rise to both high electrical conductivity and high Seebeck coefficient.^[50–56] Kim et al. prepared PEDOT:PSS films from its aqueous solution added with 5 vol% DMSO and subsequently treated them with DMSO solution of hydrazine (**Figure 5**).^[53] After hydrazine treatment, the charge concentration decreases from $\approx 4.6 \times 10^{20}$ to $\approx 2.4 \times 10^{20} \text{ cm}^{-3}$. The Seebeck coefficient

Reducing agents



P-type dopants



N-type dopants

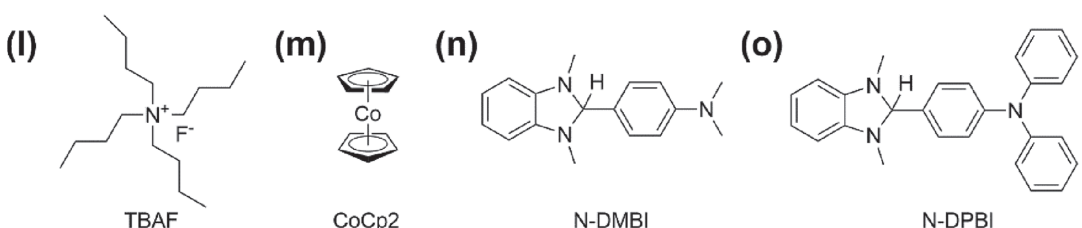


Figure 4. Chemical structures of representative reducing agents: a) HZ, b) AF, c) EMIM-BF₄, and d) TDAE; p-type dopants: e) Fetf, f) FTS, g) EBSA, h) F₄T-CNQ, i) F₂T-CNQ, j) NOPBF₆, and k) NOBF₄; n-type dopants: l) TBAF, m) CoCp₂, n) N-DMBI, and o) N-DPBI.

increases from 30 to 142 $\mu\text{V K}^{-1}$ while the electrical conductivity falls from 726 to 2 S cm^{-1} . The optimal PF is 112 $\mu\text{W m}^{-1}\text{K}^{-2}$. Later, they modified the treatment of PEDOT:PSS films by adding

both *p*-toluenesulfonic acid and DMSO into the PEDOT:PSS aqueous solution.^[54] This increases the electrical conductivity to 1218 S cm^{-1} and PF to $70.7 \mu\text{W m}^{-1} \text{ K}^{-2}$. The Seebeck coefficient

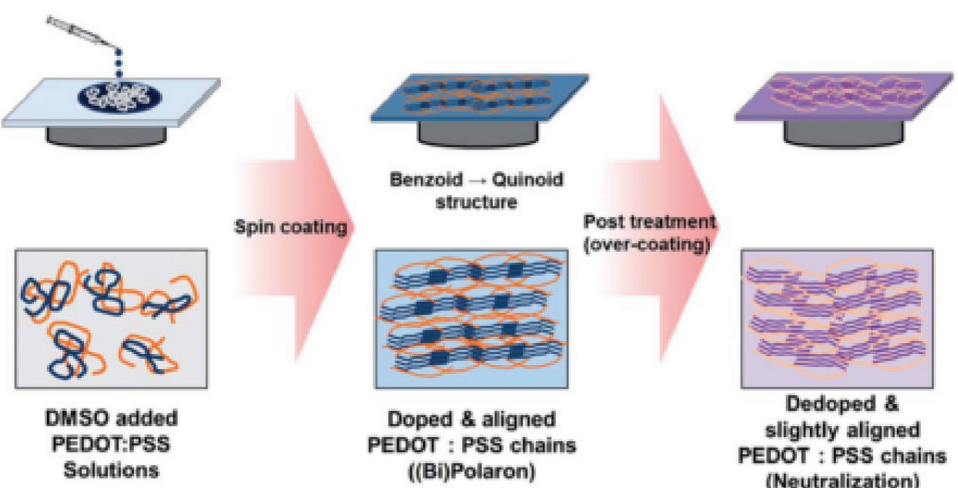


Figure 5. Schematic diagram of sequential treatments of PEDOT:PSS films. Reproduced with permission.^[53] Copyright 2014, The Royal Society of Chemistry.

**Table 2.** Summary of the TE properties of some PEDOTs doped with small counter anions.

Counterion	Treatment	$S [\mu\text{V K}^{-1}]$	$\Sigma [\text{S cm}^{-1}]$	$\text{PF} [\mu\text{W m}^{-1} \text{K}^{-2}]$	$\kappa [\text{W m}^{-1} \text{K}^{-1}]$	ZT	Ref.
TFSI ⁻	Dedoping with HZ	≈ 37	≈ 1100	147	0.19	0.22	[57]
Tos	DMF additive	35 ± 5	640 ± 10	78.5	—	—	[58]
Tos	Posttreatment with <i>p</i> -Tos	14.7 ± 0.2	1566 ± 14	33.9 ± 1.1	—	—	[59]
Tos	Posttreatment with methanol	24	1200	70	—	—	[60]
Tos	Electrochemical dedoping	≈ 117	≈ 923	1270	—	—	[61]
Tos	Dedoping with TDAE	≈ 220	≈ 67	324	—	—	[62]
Tos	Treated with NaOH	≈ 20	≈ 650	26	—	—	[63]
Tos	Treated with DMSO solution of NaBH ₄	≈ 40	≈ 580	98.1	0.451	0.064	[64]
Tos	Treated with HI	20.3	1690	69.64	0.563 (cross)	0.04	[65]

is $24.1 \mu\text{V K}^{-1}$. After the subsequent treatment with DMSO solution of HZ, the optimized PF is increased to $318.4 \mu\text{W m}^{-1} \text{K}^{-2}$ with the Seebeck coefficient of $50.4 \mu\text{V K}^{-1}$ and electrical conductivity of 1253.5 S cm^{-1} . Recently, Fan et al. investigated the post-treatments of PEDOT:PSS sequentially with acid and base.^[55,56] The acid treatment significantly enhances the electrical conductivities of the films, and the subsequent base treatment improves the Seebeck coefficient. After the sequential treatments, the Seebeck coefficient is $39.2 \mu\text{V K}^{-1}$, the electrical conductivity is 2170 S cm^{-1} , and the PF of $334 \mu\text{W m}^{-1} \text{K}^{-2}$ at room temperature. This is the highest PF achieved for PEDOT:PSS till today.

2.2. PEDOT Doped with Small Counterions

The counter anions can affect the TE properties of PEDOTs. The TE properties of some PEDOTs doped with small anions are summarized in **Table 2**. PEDOTs doped with small anions (chemical structure shown in Figure 2b) can be synthesized by electrochemical or chemical polymerization of the monomer, 3,4-ethylenedioxythiophene (EDOT). They usually exhibit higher electrical conductivity and Seebeck coefficient than as-prepared PEDOT:PSS. Their properties depend on the counter anions. Cantarero et al. investigated the effect of the counter anion size on the TE properties of PEDOT.^[57] They synthesized PEDOT doped with several counterions including ClO₄⁻, PF₆⁻ and bis(trifluoromethylsulfonyl)imide (TFSI⁻) by electrochemical polymerization. These PEDOTs exhibit conductivities in the range of $800\text{--}2120 \text{ S cm}^{-1}$. As shown in **Figure 6**, the counter anions can affect the conformation of the PEDOT chains. The large TFSI⁻ anions facilitate the PEDOT chains to have linear or expanded-coil conformation. As a result, PEDOT:TFSI shows the highest electrical conductivity of 2120 S cm^{-1} and a Seebeck coefficient of $15 \mu\text{V K}^{-1}$. They further increased the Seebeck coefficient to $42 \mu\text{V K}^{-1}$ by dedoping with hydrazine and observed an optimized PF of $147 \mu\text{W m}^{-1} \text{K}^{-2}$.

Tosylate (Tos) has often been used as the counter anion of conducting polymers because it is a surfactant with a flat benzene ring. PEDOT:Tos films can have high conductivity, and their properties can be improved through the modification of the polymerization conditions. Petsagkourakis et al. modified the polymerization of PEDOT:Tos films by adding a solvent with high boiling point like DMF into the polymerization solution.^[58] DMF can increase the crystallinity of PEDOT:Tos

and thus improve the electrical conductivity of the PEDOT:Tos films from 230 to $640 \pm 10 \text{ S cm}^{-1}$. These PEDOT:Tos films can exhibit a Seebeck coefficient of $35 \pm 5 \mu\text{V K}^{-1}$ and a PF of $78.5 \mu\text{W m}^{-1} \text{K}^{-2}$.

The TE properties of PEDOT:Tos can be enhanced through a posttreatment as well. Gong et al. investigated the treatment of PEDOT:Tos films with protonic acids.^[59] They observed the increase of the electrical conductivity from $838 \pm 17 \text{ S cm}^{-1}$ to 1329 ± 10 , 1493 ± 12 , 1507 ± 14 , and $1566 \pm 14 \text{ S cm}^{-1}$ when PEDOT:Tos films were treated with HClO₄, HCl, H₂SO₄, and *p*-toluenesulfonic acid (*p*-Tos), respectively. The conductivity enhancement is ascribed to the protonic acid doping. It is interesting that *p*-toluenesulfonic acid can give rise to the highest conductivity while it does not vary the counter anion. Thus, the Seebeck coefficient remains as $14.7 \pm 0.2 \mu\text{V K}^{-1}$ after the treatment. They reported a PF of $33.9 \pm 1.1 \mu\text{W m}^{-1} \text{K}^{-2}$ for the *p*-toluenesulfonic acid-treated PEDOT:Tos.

Organic solvents were also used to enhance the TE properties of PEDOT:Tos films.^[60] Lee et al. investigated the treatment of PEDOT:Tos films with several solvents. They found that the methanol treatment could improve the Seebeck coefficient to $\approx 24 \mu\text{V K}^{-1}$ and the electrical conductivity to $\approx 1200 \text{ S cm}^{-1}$. As a result, the PF increases from ≈ 46 to $70 \mu\text{W m}^{-1} \text{K}^{-2}$. They ascribed

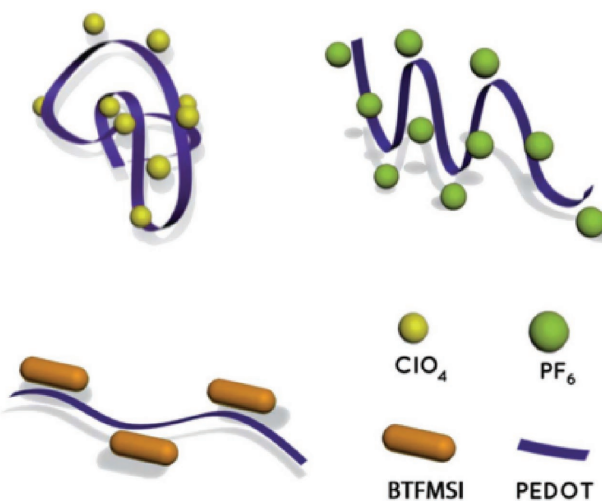


Figure 6. PEDOT conformation in the presence of different counter-ions. Reproduced with permission.^[57] Copyright 2014, The Royal Society of Chemistry.



that the improvement to the dedoping of PEDOT as revealed by the XPS spectra. The PEDOT:Tos films can be dedoped electrochemically or chemically. Park et al. electrochemically dedoped PEDOT:Tos and reported a PF of $1270 \mu\text{W m}^{-1} \text{K}^{-2}$.^[61] Although this is the highest PF for the family of PEDOT and its derivative, the reliability of this value needs further confirmation.

Chemical dedoping was also carried out by using chemical reducing agents like tetrakis(dimethylamino)ethylene (TDAE, chemical structure shown in Figure 4d), base, NaBH_4 , or HI.^[62–65] A famous work is the one by Crispin et al. who dedoped PEDOT:Tos with TDAE vapor.^[62] They observed a PF of $324 \mu\text{W m}^{-1} \text{K}^{-2}$ and ZT value of 0.25 at the doping level of 22%. Later, they also used NaOH aqueous solution to dedope PEDOT:Tos and observed a PF of $26 \mu\text{W m}^{-1} \text{K}^{-2}$.^[63] Cai et al. compared the treatments of PEDOT:Tos film with HI solution and $\text{NaBH}_4/\text{DMSO}$ solution.^[64,65] The HI treatment can give rise to an electrical conductivity of 1690 S cm^{-1} , Seebeck coefficient of $20.3 \mu\text{V K}^{-1}$, and an optimized PF of $69.6 \mu\text{W m}^{-1} \text{K}^{-2}$. In comparison, the $\text{NaBH}_4/\text{DMSO}$ treatment can lead to a higher Seebeck coefficient of $\approx 40 \mu\text{V K}^{-1}$ but a lower electrical conductivity of $\approx 600 \text{ S cm}^{-1}$. The optimized PF is $98.1 \mu\text{W m}^{-1} \text{K}^{-2}$.

2.3. Nanostructured PEDOT

Nanostructured PEDOT can exhibit high TE properties.^[66–68] Chen et al. synthesized various PEDOT nanostructures by chemical polymerization in inverse microemulsions.^[67] They found that nanostructured PEDOTs can have higher charge carrier mobility than bulk PEDOT owing to more ordered polymer chains. Among the PEDOT nanostructures, PEDOT nanofibers show the highest conductivity of 71.4 S cm^{-1} , Seebeck coefficient of $48.0 \mu\text{V K}^{-1}$ and corresponding PF of $16.4 \mu\text{W m}^{-1} \text{K}^{-2}$.

PEDOT nanowires (NWs) were also investigated as a filler in PEDOT:PSS or PEDOT:Tos. The PEDOT nanowires can tune the charge transport through the polymers by scattering the low energy carriers. At a loading of 0.2 wt% PEDOT nanowires, the composites of PEDOT:PSS and PEDOT nanowires can exhibit a Seebeck coefficient of $\approx 38.9 \mu\text{V K}^{-1}$, an electrical conductivity of $\approx 700 \text{ S cm}^{-1}$ and a PF of $\approx 102.7 \mu\text{W m}^{-1} \text{K}^{-2}$.^[68] PEDOT nanowires were also used to form composites with PEDOT:Tos by adding PEDOT nanowires into the monomer solution prior

to the polymerization. The PEDOT nanowire/PEDOT:Tos nanocomposites show a Seebeck coefficient of $59.3 \mu\text{V K}^{-1}$, an electrical conductivity of 1270 S cm^{-1} , and an extremely high PF of $446.6 \mu\text{W m}^{-1} \text{K}^{-2}$.

2.4. Polythiophene Derivatives

The TE properties of polythiophene (PTh) and its derivatives have been extensively studied. Their typical TE properties are provided in Table 3. The conductive polymer films can be prepared by electrochemical or chemical polymerization of the corresponding monomers. They can also be fabricated by processing the polymers in neutral state followed by doping.

2.4.1. TE Properties of Polythiophenes by Electrochemical Polymerization

Electrochemical polymerization is a popular way to prepare films of PTh and its derivatives. The properties of the polymer films, such as the electrical conductivity and Seebeck coefficient, depend on the polymerization conditions. Shinohara et al. found that the electrical conductivity of PTh was more sensitive to the experimental conditions than its Seebeck coefficient.^[69] The PTh films with high crystallinity can exhibit an electrical conductivity of 201 S cm^{-1} and PF of $10.3 \mu\text{W m}^{-1} \text{K}^{-2}$. Xu et al. modified the electrochemical polymerization conditions of PTh, poly(3-methylthiophene) (P3MeT), and poly(3-octylthiophene) (P3OT) by adding 2,6-di-*tert*-butylpyridine (DTBP, chemical structure shown in Figure 2c) into the polymerization solution.^[70] DTBP works as a proton scavenger, and it can lower the solution acidity and suppress the acid-initiated side reactions. As a result, it increases the conjugated length and interchain packing of the polymers. They observed an electrical conductivity of 65.9 S cm^{-1} , Seebeck coefficient of $36.7 \mu\text{V K}^{-1}$ and a PF of $8.88 \mu\text{W m}^{-1} \text{K}^{-2}$.

2.4.2. PTh Derivatives by Postdoping

Many PTh derivatives are soluble in organic solvents when in neutral state while insoluble when in oxidized state. Their

Table 3. Summary of the TE properties of some typical polythiophene derivatives.

Polymer	Dopant	Treatment	$S [\mu\text{V K}^{-1}]$	$\Sigma [\text{S cm}^{-1}]$	$\text{PF} [\mu\text{W m}^{-1} \text{K}^{-2}]$	Ref.
Polythiophene	ClO_4^-		23	201	10.3	[69]
Polythiophene	–		42.5	65.9	8.88	[70]
P3HT	TFSI ⁻	Immerse doping	≈ 48	≈ 87	≈ 20	[72]
PBTTC14	FTS	Vapor doping	23 ± 4	466.0 ± 0.1	25 ± 8	[73]
PBTTC14	FTS	Vapor doping	33 ± 5	1000 ± 70	110 ± 34	[74]
PBTTC14	F ₄ TCNQ	Vapor doping	42	670	120	[75]
PDPP3T	FeCl_3	Spin-coating doping	226	55	276	[76]
PDPP3T	TFSI ⁻	Immerse doping	45	62	25	[77]
PDTDE12	F ₄ TCNQ	Drop doping	≈ 30	120	≈ 10	[78]



conductive films are thus prepared by processing the solutions of the polymers in neutral state and postoxidization.^[71–79] For example, Zhu et al. oxidized poly(3-hexylthiophene) (P3HT) films with ferric(III) triflimide ($\text{Fe}(\text{TSI})_3$, chemical structure shown in Figure 4e) solution and observed a PF over $20 \mu\text{W m}^{-1} \text{K}^{-2}$.^[72]

The doping process and dopant can saliently affect the TE properties. Chabiny's lab carried out a systematic study on the postdoping of PTh derivatives. They doped P3HT, poly(2,5-bis(3-tetradearylthiophen-2-yl)thieno[3,2-b]thiophene) (PBTTTC14, chemical structure shown in Figure 2d) and poly(2,5-bis(thiophen-2-yl)-(3,7-diheptadecanylthienoacene)) (P2TDC17-FT4, chemical structure shown in Figure 2e) with fluoroalkyl trichlorosilanes (FTS, chemical structure shown in Figure 4f) or F_4TCNQ .^[73] They discovered that FTS can give rise to higher electrical conductivity and PF than F_4TCNQ . For example, PBTTTC14 doped with F_4TCNQ shows an electrical conductivity of only $3.51 \pm 0.05 \text{ S cm}^{-1}$ and PF of $1.3 \pm 0.4 \mu\text{W m}^{-1} \text{K}^{-2}$, while the one doped with FTS exhibits an electrical conductivity of $604.0 \pm 0.7 \text{ S cm}^{-1}$ and PF of $22 \pm 7 \mu\text{W m}^{-1} \text{K}^{-2}$. Later, they investigated the doping of PBTTTC14 with 4-ethylbenzenesulfonic acid (EBSA, chemical structure shown in Figure 4g) solution or FTS vapor.^[74] PBTTTC14 doped with EBSA can show a Seebeck coefficient of $\approx 14 \mu\text{V K}^{-1}$ and PF of $\approx 25 \mu\text{W m}^{-1} \text{K}^{-2}$, while the one doped with FTS can have a Seebeck coefficient of $\approx 33 \mu\text{V K}^{-1}$ and PF of $\approx 100 \mu\text{W m}^{-1} \text{K}^{-2}$. They studied the polymer microstructure with grazing incident wide-angle X-ray scattering (GIWAXS) and proposed that the dopants could give rise to disordered structure and thus affect the Seebeck coefficient. In further study, they investigated the doping of PBTTTC14 with F_4TCNQ or F_2TCNQ in vapor or solution state.^[75] The chemical structures of F_4TCNQ and F_2TCNQ are shown in Figure 4h,i. They found that the vapor doping could yield higher electrical conductivity than the solution doping. PBTTTC14 doped with F_4TCNQ vapor exhibits an electrical conductivity of $670 \pm 4 \text{ S cm}^{-1}$, a Seebeck coefficient of $42 \pm 6 \mu\text{V K}^{-1}$, and a PF of $120 \pm 30 \mu\text{W m}^{-1} \text{K}^{-2}$. In comparison, F_2TCNQ gives rise to a higher Seebeck coefficient of $140 \pm 20 \mu\text{V K}^{-1}$ but low electrical conductivity of $36 \pm 3 \text{ S cm}^{-1}$. The PF of PBTTTC14 doped with F_2TCNQ is thus only $70 \pm 20 \mu\text{W m}^{-1} \text{K}^{-2}$. F_2TCNQ is a weak acceptor, it cannot dope the polymer effectively.

2.4.3. PTh Derivatives of Different Chemical Structures

Apart from the counter ions and the doping level, the TE properties of polymers depend on the chemical structure. Generally, polymers with high charge carrier mobility can have high PF. For example, Jung et al. studied poly(diketopyrrolopyrrole-terthiophene) (PDPP3T, chemical structure shown in Figure 2f) that has high carrier mobility due to the large planar structure.^[76] They observed an optimal PF of $276 \mu\text{W m}^{-1} \text{K}^{-2}$ for PDPP3T doped by iron (III) chloride.

The TE properties are sensitive to the conjugated structure of the polymer chains. Zhu et al. did a comparative study on several polymers with different charge carrier mobilities, including poly(2,5-bis(3-dodecylthiophen-2-yl)-thieno[3,2-b]thiophene) (PBTTTC12, chemical structures shown in Figure 2d), poly[2,5-bis(2-hexyldecyl)-2,3,5,6-tetrahydro-3,6-dioxopyrrolo[3,4-c]pyrrole-1,4-diyl]-alt-[{2,2':5',2"-terthiophene}-5,5"-diyl] (PDPP3T) and poly[(4,4'-bis(2-ethylhexyl)dithieno[3,2-b:2',3-d]silole)-2,6-diyl-alt-(2,1,3 benzothiadiazole)-4,7-diyl] (PSBTBT, chemical structures shown in Figure 2g).^[77] The optimal PFs of PDPP3T, PBTTTC12, and PSBTBT are 25, 14, and $3.5 \mu\text{W m}^{-1} \text{K}^{-2}$, respectively. They investigated the charge carrier mobility of these polymers and ascribed their different PFs to the chemical structure and microstructure. Among these polymers, heavily doped PBTTTC12 has the highest mobility of $1.6 \text{ cm}^2 \text{ V}^{-1} \text{ s}^{-1}$ and thus the highest conductivity of 200 S cm^{-1} . But it has the lowest Seebeck coefficient of $13 \mu\text{V K}^{-1}$.

The TE properties can be affected by the side groups of the conjugated polymer chains. Katz et al. synthesized PQTS12, PDTDE12, and PDTDES12 by introducing sulfur atoms or ethylenedioxy to the side groups of poly(bisododecylquaterthiophene) (PQT12) (Figure 7).^[78] The sulfur atoms and the ethylenedioxy groups can raise the highest occupied molecular orbital (HOMO) level of the conjugated polymers and thus facilitate the oxidation of the conjugated backbone. They can also affect the planarity of the conjugated unit and thus the packing of the backbone. The HOMO levels of the PQT12, PQTS12, PDTDE12, and PDTDES12 are -5.09 , -5.04 , -4.83 , and -4.67 eV, respectively. These four polymers were doped with F_4TCNQ or nitrosonium tetrafluoroborate (NOBF_4 , chemical structure shown in Figure 4k). The doping level generally increases with

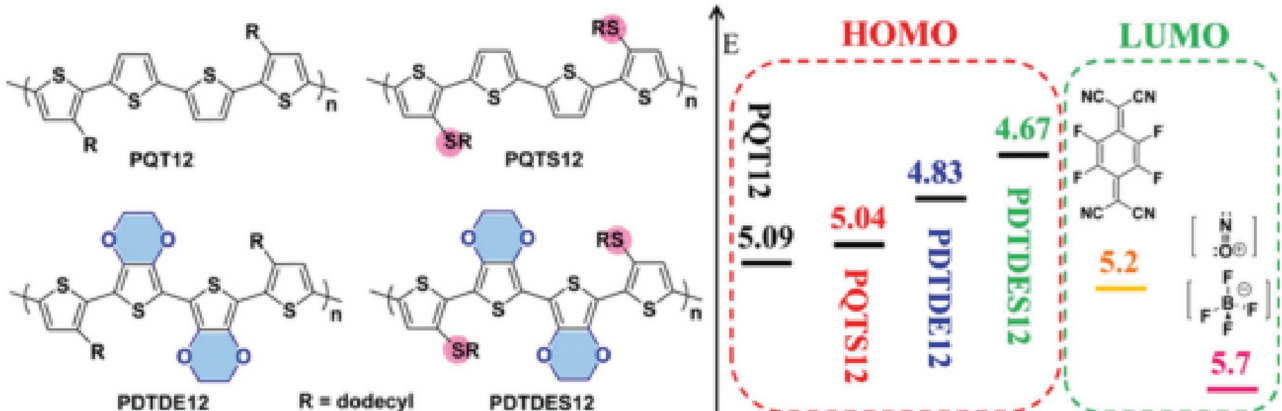


Figure 7. Chemical structures of polymers and dopants and their HOMO and LUMO energy levels, respectively. Reproduced with permission.^[78] Copyright 2017, The American Chemical Society.



the rising HOMO level except PDTDES12. Apart from the doping level, the microstructure of the polymers also affects the electrical conductivity. The sulfur atoms has negligible effect on the planarity, but ethylenedioxy group can have steric effect on the conjugated structure. Hence, the PQTS12 films have highly ordered packing structure, while the backbone of PDTDE12 and PDTDES12 is distorted. In addition, the dopants can affect the microstructure of the polymers. NOBF_4 can make the conjugated backbones pack more closely than F_4TCNQ , leading to higher electrical conductivity.

2.4.4. Blends of PTh Derivatives

Charge transfer may take place when two polymers with different Fermi levels are blended together. This will affect both the electrical conductivity and the Seebeck coefficient. Katz et al. designed such a system by mixing a small amount of poly(3-hexylthiophiophene) (P3HTT) into P3HT.^[79] They then doped the polymer blend with F_4TCNQ . The hole energy of P3HT is slightly higher than that of P3HTT due to the deeper HOMO level. As a result, the holes on P3HT will be transferred to P3HTT. When the doping level is not high, the majority of the holes will be on the P3HTT chains. Thus, the Seebeck coefficient of P3HT is high due to the low hole concentration on it. By this way, the blend can have high Seebeck coefficient while acceptable conductivity. Within the P3HTT loading of 8–20 wt%, both electrical conductivity and Seebeck coefficient of the polymer blends increase with the increasing P3HTT loading. The optimal PF of the PTh blends is $7.58 \times 10^{-3} \mu\text{W m}^{-1} \text{K}^{-2}$.

2.5. Other p-Type TE Polymers

The TE properties of other conductive polymers, including PANI, PPV, PPy, polycarbazole, and their derivatives, were investigated as well. Their TE properties are summarized in Table 4. PANI usually exhibits low Seebeck coefficient and low electrical conductivity.^[80–85] For example, the hydrochloric acid-doped PANI shows a low conductivity of $\approx 1.5 \text{ S cm}^{-1}$, a Seebeck coefficient of $\approx 40 \mu\text{V K}^{-1}$, and a corresponding PF of $\approx 0.24 \mu\text{W m}^{-1} \text{K}^{-2}$. The ZT value is only 2.67×10^{-4} .^[85] The TE properties can be improved by mechanically aligning the polymer chains. Toshima et al. found that PANI:CSA (CSA for camphorsulfonic acid, chemical structures shown in Figure 2h) films can

show a PF of $5 \mu\text{W m}^{-1} \text{K}^{-2}$ after mechanical stretching.^[83] The mechanical stretching makes the polymer chains more oriented and thus increase the charge carrier mobility. The TE properties of PANI also depend on its microstructure. Zhu et al. reported that the nanotube structure of PANI could increase its charge carrier mobility and thus the electrical conductivity and Seebeck coefficient.^[84] They observed a Seebeck coefficient of $31.3 \mu\text{V K}^{-1}$ and a conductivity of $4.5 \times 10^{-3} \text{ S cm}^{-1}$ for normal PANI. In contrast, the PANI nanotubes show a much higher Seebeck coefficient of $212.4 \mu\text{V K}^{-1}$ and a conductivity of $7.7 \times 10^{-3} \text{ S cm}^{-1}$. The PF of PANI is generally very low due to its low electrical conductivity.

PPV derivatives can have much higher Seebeck coefficient than PANI.^[86,87] For example, the iodine-doped P(EtOPV-co-PV) whose chemical structure is shown in Figure 2i exhibits an electrical conductivity of 349.2 S cm^{-1} , Seebeck coefficient of $47.3 \mu\text{V K}^{-1}$ and PF of $78.1 \mu\text{W m}^{-1} \text{K}^{-2}$. The ZT value is 9.87×10^{-2} .

The TE properties of PPy (chemical structures shown in Figure 2j) was studied as well. The major efforts were made on PPy nanostructures. Zhang et al. investigated the TE performance of PPy films consisting of PPy nanotubes with different sizes.^[88] They found that longer PPy nanotubes can lead to higher TE properties. The PPy film consisted of shorter PPy nanotubes shows an electrical conductivity of 3.43 S cm^{-1} , Seebeck coefficient of $16.51 \mu\text{V K}^{-1}$, and PF of $0.09 \mu\text{W m}^{-1} \text{K}^{-2}$. In comparison, the PPy films made up with longer PPy nanotubes exhibit an electrical conductivity of 9.81 S cm^{-1} , Seebeck coefficient of $17.68 \mu\text{V K}^{-1}$ and PF of $0.31 \mu\text{W m}^{-1} \text{K}^{-2}$. The TE properties also depend on the structure of the nanostructured PPy. Guo et al. prepared different PPy nanostructures including nanowires and nanoparticles by tuning the polymerization condition.^[89] They found that the nanowires with large aspect ratio exhibited the highest PF of $(22.6 \pm 3.6) \times 10^{-3} \mu\text{W m}^{-1} \text{K}^{-2}$.

Compared with PANI and PPy, polycarbazole derivatives usually exhibit high Seebeck coefficients but low electrical conductivity.^[90–93] This is attributed to the charge localization on the nitrogen atom. The introduction of vinylene and electron-donating unit like thiophene or bis(3,4-ethylenedioxythiophene) can significantly increase the conductivity of the polycarbazole derivatives. An electrical conductivity up to 160 S cm^{-1} , Seebeck coefficient of $34 \mu\text{V K}^{-1}$, and a corresponding PF of $19 \mu\text{W m}^{-1} \text{K}^{-2}$ were reported for a polycarbazole derivative (PCDTBT, chemical structure shown in Figure 2k).^[92]

Table 4. Summary of the TE properties of PANI, PPy, PA, and polycarbazole.

Polymer	Dopant	$S [\mu\text{V K}^{-1}]$	$\sigma [\text{S cm}^{-1}]$	$\text{PF} [\mu\text{W m}^{-1} \text{K}^{-2}]$	$\kappa [\text{W m}^{-1} \text{K}^{-1}]$	ZT	Ref.
PANI	CSA ⁻	5	160	0.4	—	—	[80]
PANI nanotube	β -Naphthalene sulfonic acid	212.4	0.0077	0.035	0.21	—	[84]
PANI nanotube	HCl	≈ 8	≈ 530	≈ 3	0.276	0.4×10^{-4}	[85]
P(EtOPV-co-PV)	I ₂	47.3	349.2	78.1	0.25	9.87×10^{-2}	[87]
PPy nanotube	HCl	17.68	9.81	0.31	0.17	5.7×10^{-4}	[88]
PPy nanowire	SO ₄ ²⁻	10.1 ± 0.1	2.21 ± 0.30	$(22.6 \pm 3.6) \times 10^{-3}$	—	—	[89]
PCDTBT	FeCl ₃	34	160	19	—	—	[92]
PA	I ₂	15	60 000	1350	—	—	[94]



Among the conductive polymers, PA (chemical structures shown in Figure 2l) has the simplest conjugated structure. When the polymer chains are well aligned, it can have high crystallinity and thus high electrical conductivity. The iodine-doped PA can display an ultrahigh electrical conductivity of up to $60\,000\text{ S cm}^{-1}$ and a very high PF of up to $1350\text{ }\mu\text{W m}^{-1}\text{ K}^{-2}$.^[94] However, it does not have any practical significance due to its extremely poor environmental stability.

3. n-Type Polymers

Both p-type and n-type materials are required to compose an efficient TE generator or Peltier cooler. Regardless of the intensive study on p-type organic TE materials, the development of n-type counterpart is more challenging due to their poor air stability.

3.1. n-Type Organic Polymers

The stability of n-type polymers is related to the lowest unoccupied molecular orbital (LUMO). To have good stability in ambient condition, the n-type polymers should have a deeper LUMO. The LUMO level can be lowered by introducing electron-withdrawing units in the backbone or as side groups. A couple of n-type organic small molecules were reported, such as naphthalenetetracarboxylic dianhydride,^[95] benzotriazole,^[96] perylene bisimide,^[97] naphthodithiophenediimide,^[98] and fullerenes.^[99] Organic donor molecules, such as 4-(1,3-dimethyl-2,3-dihydro-1*H*-benzimidazol-2-yl)phenyl)dimethylamine (N-DMBI),^[100] tetra-*n*-butylammonium fluoride (TBAF),^[101] and cobaltocene (CoCp_2),^[102] were employed to dope these n-type molecules. The chemical structures of these dopants are shown in Figure 4l–n.

The TE properties of some n-type polymers are presented in Table 5.^[103–113] As early as in 1981, Heeger's lab reported n-type polyacetylene doped with TBAF by electrochemical reduction.^[106] They observed a Seebeck coefficient of $-43.5\text{ }\mu\text{V K}^{-1}$. But it was extremely unstable. In 2013, Pei and co-workers introduced electron withdrawing elements like Cl and F to *p*-phenylene vinylene (PPV).^[107] The fluorine functionalized benzodifuranone-based poly(*p*-phenylene vinylene) (FBDPPV, chemical structure shown in Figure 8a) doped with N-DMBI can have a PF of $28\text{ }\mu\text{W m}^{-1}\text{ K}^{-2}$.^[108] The TE properties of n-type polymers also depend greatly on the morphology. Ma et al. investigated the effect of dopant on the crystallinity

on FBDPPV.^[109] The GIWAXS results indicate that the crystallinity of the polymer varies with the doping level of N-DMBI. FBDPPV with the optimal doping level can exhibit an electrical conductivity of 6.2 S cm^{-1} , a Seebeck coefficient of $-210\text{ }\mu\text{V K}^{-1}$ and a power factor of $25.5\text{ }\mu\text{W m}^{-1}\text{ K}^{-2}$.

Similar to the PPV derivatives, poly{*N,N'*-bis(2-octyl-dodecyl)-1,4,5,8-naphthalenedicarboximide-2,6-diyl]-alt-5,5-(2,2-bithiophene)} (P(NDIOD-T2), chemical structure shown in Figure 8b) with the electron-deficient imidazole groups can be n-type thermoelectric polymers. Chabiny et al. investigated this polymer with different dopants, including 4-(1,3-dimethyl-2,3-dihydro-1*H*-benzimidazol-2-yl)-*N,N*-diphenylaniline (N-DPBI, chemical structure shown in Figure 4o) and N-DMBI.^[114] PNDIOD-T2 doped with N-DMBI can show a PF of $0.6\text{ }\mu\text{W m}^{-1}\text{ K}^{-2}$, higher than the one doped with N-DPBI. The PNDIOD-T2 polymers in the doped state show better air stability than PPV derivatives. Additionally, they can be dispersed in organic solvents like 1,2-dichlorobenzene and can be thus processed by solution processing techniques. Inspired by PVDIOD-T2, copolymers of naphtho[2,3-b:6,7-b]dithiophenediimide (NDTI) and benzobisthiadiazole (BBT) units like PNNDTI-BBT-DT and PNNDTI-BBT-DP (chemical structures are shown in Figure 8c) were synthesized.^[115] They exhibit an electrical conductivity of 5 S cm^{-1} and a PF of $14\text{ }\mu\text{W m}^{-1}\text{ K}^{-2}$.

Conjugated polymers with ladder structures can have high solubility in organic solvents. They were investigated as n-type TE polymers. Ladder-type polymers such as polybenzimidazobenzophenanthroline (BBL, chemical structure shown in Figure 8d) doped with TDAE was reported.^[116] Although its PF is only $0.43\text{ }\mu\text{W m}^{-1}\text{ K}^{-2}$, it is soluble in organic solvents like o-dichlorobenzene. Hence, it can be processed in large scale like the p-type PEDOT:PSS.

Some polymers with a low bandgap can be both n-type or p-type materials. For example, poly-peri-naphthalene (PPN, chemical structure shown in Figure 8e) has an ultralow bandgap ranging from 0.035 to 0.13 eV . It shows p-type behavior at room temperature, but behaviors as an n-type material at elevated temperature arising from the thermal excitation of electrons.^[117]

3.2. Metal–Organic Hybrid n-Type Polymers

Conjugated polymers with metal atoms in the backbone can show n-type behavior and have good air stability.^[118–122] A good example is poly(nickel-ethylenetetrathiolate) (K_xNiEt_4 , chemical

Table 5. Summary of the TE properties of some typical n-type polymers.

Polymer	Dopant	$S\text{ [}\mu\text{V K}^{-1}\text{]}$	$\sigma\text{ [S cm}^{-1}\text{]}$	$\text{PF [}\mu\text{W m}^{-1}\text{ K}^{-2}\text{]}$	$\kappa\text{ [W m}^{-1}\text{ K}^{-1}\text{]}$	ZT	Ref.
PA	Bu ₄ N	-43.5	5	1	-	-	[106]
FBDPPV	DMBI	-141	14	28	-	-	[108]
FBDPPV	DMBI	-210	6.2	25.5	-	-	[109]
P(NDIOD-T2)	DMBI	-850	0.008	0.6	-	-	[114]
BBL	TDAE	-101	0.42	0.43	-	-	[116]
K _x NiEt ₄	N. A.	-126	40	66	-0.2	~0.1	[112]
K _x NiEt ₄	N. A.	-90	210	170	0.4–0.5	0.30	[113]
CuBHT	N. A.	-4 to -10	750–1580	N. A.	-	-	[111]

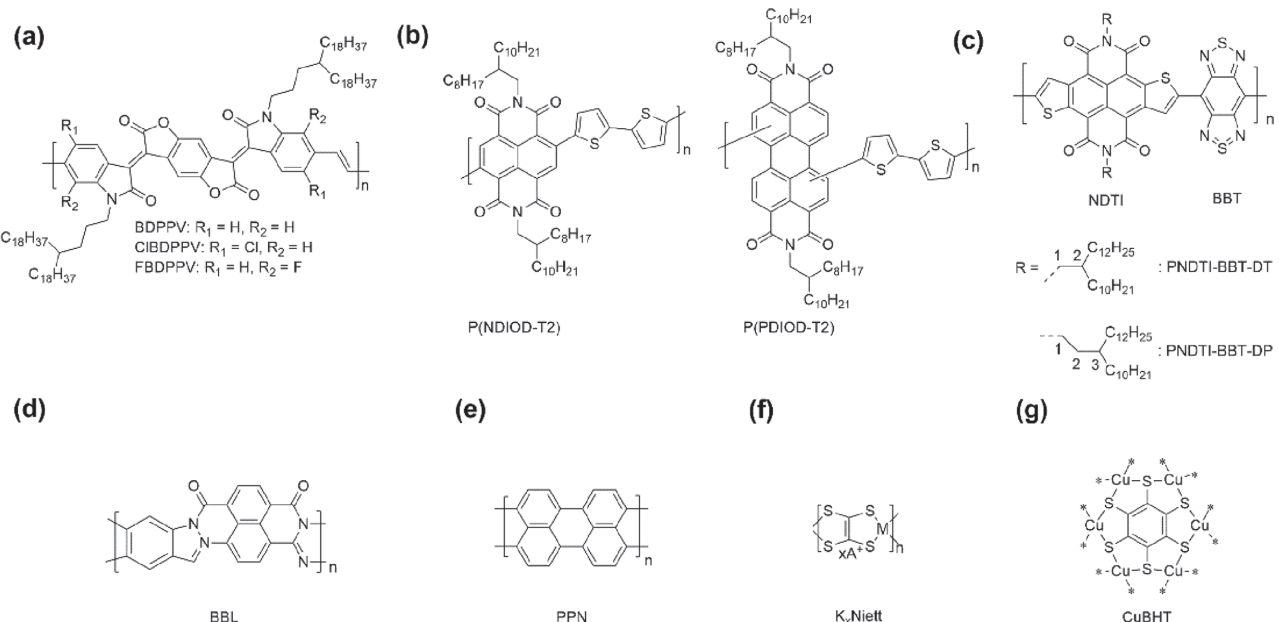


Figure 8. Chemical structures of n-type polymers: a) FBDPPV, b) P(NDIOD-T2), c) PNNDTI-BBT-DT and PNNDTI-BBT-DP, d) BBL, e) PPN, f) K_x Niett, and g) CuBHT.

structure shown in Figure 8f). Its electronic structure and properties can be tuned by adopting different central metallic ions and counter cations. Zhu's lab reported the preparation of K_x Niett films by electrochemical polymerization.^[122] They observed a PF of $162 \mu\text{W m}^{-1} \text{K}^{-2}$, which is much higher than other n-type conjugated polymers or small molecules.^[113] Furthermore, TE generators were built by using K_x Niett films. A device with an array of 108 K_x Niett single legs could exhibit a power output of $577.8 \mu\text{W cm}^{-2}$.^[123] Besides K_x Niett, the TE performance of other polymers with the Ni–S coordinate bonds, such as copper benzenehexathiol complex (Cu-BHT, chemical structure shown in Figure 8g), was investigated.^[111] Cu-BHT can have a high electrical conductivity over 1500 S cm^{-1} and a Seebeck coefficient of -4 to $-10 \mu\text{V K}^{-1}$.

4. Composites

Composites of a polymer and nanomaterials can exhibit high TE properties. The interaction between nanofillers and polymer matrix can often yield decoupled TE parameters, thereby leading to significantly enhanced PF compared with individual components. In addition, the filler/polymer interface creates numerous boundaries that suppress the phonon transport by phonon scattering, ensuring the composites a low thermal conductivity.

The fillers of TE composites can be either inorganic or organic, while the matrix can be either insulating or intrinsically conductive. In 2008, Grunlan et al. demonstrated the great potential of CNT/poly(vinyl acetate) (PVAc) composites for TE applications.^[124] They found that as long as the CNT fillers formed percolation in the insulating matrix, the electrical conductivity of the composites could be dramatically increased while their thermal conductivity and Seebeck coefficient remained insensitive to the filler concentration. At the

CNT loading of 20 wt%, the CNT/PVAc composites exhibit an electrical conductivity of 48 S cm^{-1} , Seebeck coefficient of $40 \mu\text{V K}^{-1}$ and thermal conductivity of $0.34 \text{ W m}^{-1} \text{K}^{-1}$. Although the electrical conductivity was increased by several orders of magnitude with the addition of CNTs, the Seebeck coefficient and thermal conductivity of the composites are close to those of the matrix. As a result, the composite can have a ZT value of 0.006. Other than PVAc, other insulating polymers have also been employed as the matrix. However, as most of the insulating polymers contribute little to the conductivity, their composites usually suffer from low electrical conductivity. For instance, the electrical conductivity of a few-layer graphene/PVDF composite achieved only 21 S cm^{-1} even at a very high graphene loading of 80%.^[125] Hence, the PF of these insulating polymer-based composites is usually below $10 \mu\text{W m}^{-1} \text{K}^{-2}$. Thus, intrinsically conductive polymers are preferred as the matrix of TE composites.

4.1. Composites with Inorganic TE Fillers

Inorganic TE materials like PbTe or Bi_2Te_3 can exhibit a high ZT value.^[126–128] They were adopted as the nanofillers in TE composites. The TE properties of some polymer composites with inorganic TE materials are provided in Table 6. Segalman et al. prepared TE composites by in situ synthesis of Te nanorods in PEDOT:PSS aqueous solution.^[129] The Te nanorod/PEDOT:PSS composites can exhibit a PF of up to $70.9 \mu\text{W m}^{-1} \text{K}^{-2}$ and a low thermal conductivity of 0.22 – $0.3 \text{ W m}^{-1} \text{K}^{-1}$. In comparison, the PFs of Te nanorods and PEDOT:PSS are only 2.7 and $0.05 \mu\text{W m}^{-1} \text{K}^{-2}$, and their thermal conductivities were 2 and 0.24 – $0.29 \text{ W m}^{-1} \text{K}^{-1}$, respectively. The improvement in the TE properties was ascribed to the carrier filtering and phonon scattering effects, arising from the nanoscale inorganic/organic interfaces.^[130]

**Table 6.** Summary of the TE properties of polymer composites with inorganic TE materials.

Polymers	Fillers	Synthesis method	Loading [wt%]	$S [\mu\text{V K}^{-1}]$	$\sigma [\text{S cm}^{-1}]$	$\text{PF} [\mu\text{W m}^{-1} \text{K}^{-2}]$	$\kappa [\text{W m}^{-1} \text{K}^{-1}]$	ZT	Ref.
PEDOT:PSS	Te NWs	In situ synthesis	–	163	19.3	70.9	0.22–0.30 ^{a)}	≈0.1	[129]
PEDOT:PSS	Te NWs	In situ synthesis	–	180	11	35	0.16 ^{a)}	≈0.07	[130]
PEDOT:PSS	Te NWs	In situ synthesis + H_2SO_4 treatment	–	115	215	284	0.22 ^{b)}	0.39	[42]
PEDOT:PSS	$\text{Bi}_2\text{Te}_3^{\text{c})}$	Drop casting PEDOT:PSS on Bi_2Te_3 layer	–	145 (p-type)	62	131	≈0.5 ^{b)}	≈0.08	[139]
			–	–125 (n-type)	50	80			
PEDOT:PSS	Bi_2Te_3	Solution mixing	4.1	16	1295	32.26	0.2 ^{b)}	≈0.05	[140]
PEDOT:PSS	$\text{Bi}_{0.5}\text{Sb}_{1.5}\text{Te}_3$	Solution mixing	30	130	≈5	8.5	0.3 ^{a)}	≈0.01	[141]
PEDOT:PSS	MoS_2	Solution mixing	4	19.5	1250	45.6	0.27 ^{a)}		[143]
PEDOT:PSS	SnSe	Solution mixing	20	110	320	380	0.36 ^{a)}	0.32	[142]
PANI	Te	Solution mixing	70	102	102	105	≈0.21	0.156	[144]
PANI	Bi_2Te_3	In situ polymerization	30	40	11.6	≈2	0.11	0.004	[146]
P3HT	Bi_2Te_3	Solution mixing	20	117	10	13.6	0.86 ^{a)}	–	[133]
PVDF	Ni NWs	Solution mixing	80	–20	4701	200	0.55	≈0.15	[151]

^{a)}Measured thermal conductivity; ^{b)}Calculated thermal conductivity; ^{c)} Bi_2Te_3 carrier type can be determined by the precise stoichiometry of atoms. NWs = nanowires.

Rational engineering of the inorganic/organic interfaces is important to achieve high TE performance for composites.^[131,132] Qiu et al. carried out a comprehensive study on the energy filtering effect on the TE properties of Bi_2Te_3 /P3HT composites.^[133] By altering the doping level of P3HT, the interfaces with different energy barriers between Bi_2Te_3 and P3HT are created. An appropriate interfacial potential barrier can selectively scatter low-energy carriers and transport high-energy carriers across the interfaces.^[134] The low-energy carriers occupying the DOS below the Fermi level can negatively contribute to the Seebeck coefficient. Therefore, filtering out these low-energy carriers by the interfaces can enhance the average energy of the carriers in the material.^[135] Subsequently, the DOS in the composites can be sharpened due to the redistribution of carrier energy, thus leading to significantly enhanced Seebeck coefficient while keeping the electrical conductivity constant in large extent.

The electrical conductivity and the Seebeck coefficient are interdependent as shown in **Figure 9**. When the electrical conductivity of P3HT and the Bi_2Te_3 /P3HT composites are below 2 S cm^{-1} , the Seebeck coefficient and PF of the composites are slightly lower than those of the neat P3HT, implying that the enhanced TE properties are not simply due to the physical inclusions of Bi_2Te_3 . To maximize energy filtering effect, the ideal loading of the inorganic fillers should be below or near the percolation threshold, where only a thin layer (nanometer or possibly even micrometers thick) of polymer coats on the inorganic fillers.^[136] On the other hand, phonon scattering has been addressed earlier for nanostructured inorganic materials, such as superlattices.^[137,138] Conventional inorganic TE materials like Bi_2Te_3 and Te NWs usually possess thermal conductivities of $1.2\text{--}2.8 \text{ W m}^{-1} \text{ K}^{-1}$,^[129,139] nearly one order of magnitude greater than most conducting polymers.^[7,132] However, owing to the numerous interfaces in the inorganic/organic composites

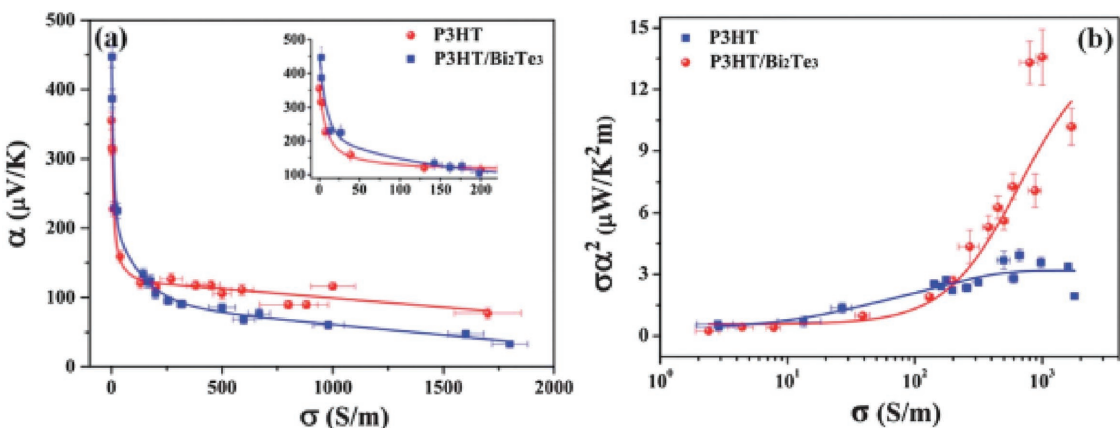


Figure 9. Correlation between a) Seebeck coefficient and electrical conductivity, and b) PF and electrical conductivity of P3HT and P3HT- Bi_2Te_3 nanocomposites. Reproduced with permission.^[133] Copyright 2012, The Royal Society of Chemistry.



that also scatter phonons, the TE composites have a low thermal conductivity close to that of the polymer matrix. It has been reported that the thermal conductivity of the TE composites is insensitive to the filler loadings.^[129,130]

Such enhanced electron transport and diminished phonon transport by engineering the inorganic/organic interfaces have also been reported for other composites, such as Bi₂Te₃/PEDOT:PSS,^[139,140] Bi_{0.5}Sb_{1.5}Te₃/PEDOT:PSS,^[141] SnSe/PEDOT:PSS,^[142] MoS₂/PEDOT:PSS,^[143] Te/PANI,^[144] MoS₂/PANI,^[145] Bi₂Te₃/PANI,^[146] and MoS₂/PPy.^[147] For instance, Katz et al. incorporated both p- and n-type Bi₂Te₃ powders into PEDOT:PSS matrix by drop casting PEDOT:PSS solutions on predeposited Bi₂Te₃ films (Figure 10a,b).^[139] PFs for the p- and n-type composites were enhanced to 131 and 80 $\mu\text{W m}^{-1} \text{K}^{-2}$, respectively, 2–3 folds higher than that of the neat PEDOT:PSS ($\sim 47 \mu\text{W m}^{-1} \text{K}^{-2}$). Urban et al. developed Te-Cu_{1.75}Te/PEDOT:PSS TE composites by controlled patterning of Cu–Te alloy subphases in hybrid PEDOT:PSS–Te nanowires (Figure 10c).^[148] At the optimal conditions, an enhancement of the PF from 69 to 84 $\mu\text{W m}^{-1} \text{K}^{-2}$ was successfully obtained. Kim et al. prepared composites of SnSe nanosheets (NSs) and PEDOT:PSS (Figure 10d–g).^[142] A high PF of 380 $\mu\text{W m}^{-1} \text{K}^{-2}$ and a ZT value of 0.32 were obtained for the composites at a SnSe loading of 20 wt%.

In order to estimate the upper and lower limits of the TE parameters in a binary TE composite, parallel and series models are widely adopted to describe its Seebeck coefficient with the electrical conductivity and thermal conductivity as a function of the filler loading. These two models can be interpreted as the two phases of a binary composite, i.e., fillers and matrix. Arranged in parallel and series with respect to the conduction flow, they basically provide the upper and lower limits of the effective material property. Although the interfaces are important, they are neglected in these two models. A basic guideline

can be roughly provided for designing the inorganic-organic composites. Equations of these two models are given as below

$$\sigma_{c,s}^{-1} = (1 - x_f) \cdot \sigma_m^{-1} + x_f \cdot \sigma_f^{-1} \quad (1)$$

$$\sigma_{c,p} = (1 - x_f) \cdot \sigma_m + x_f \cdot \sigma_f \quad (2)$$

$$S_{c,s} = [(1 - x_f) \cdot S_m / \kappa_m + x_f \cdot S_f / \kappa_f] / [(1 - x_f) / \kappa_m + x_f / \kappa_f] \quad (3)$$

$$S_{c,p} = [(1 - x_f) \cdot \sigma_m \cdot S_m + x_f \cdot \sigma_f \cdot S_f] / [(1 - x_f) \cdot \sigma_m + x_f \cdot \sigma_f] \quad (4)$$

where $\sigma(S)_{c,s}$, $\sigma(S)_{c,p}$, x_f , $\sigma(S)_m$, $\sigma(S)_f$, κ_m , and κ_f are the electrical conductivity (Seebeck coefficient) of the series-connected composite, parallel-connected composite, volume fraction of the fillers, electrical conductivity (Seebeck coefficient) of the polymer matrix, electrical conductivity (Seebeck coefficient) of the fillers, thermal conductivity of the matrix, and thermal conductivity of the fillers, respectively. The upper and lower limits of the PFs of the TE composites can accordingly be given by the products of these two models.^[139] As shown in Figure 11, the electrical conductivity of the SnSe/PEDOT:PSS composites lie well in between the series and parallel models, whereas the Seebeck coefficients exhibit enhanced values compared with the expected models.^[142] This is due to the interfacial effects for TE composites.

In spite that great enhancement has been achieved on the Seebeck coefficients, there is still room for the improvement of the electrical conductivity of the inorganic/organic TE composites. In several works, the conductivities of the composites appeared to be unsatisfactory, sometimes even lower than either the inorganic fillers or the polymeric matrix.^[139] Methods to effectively reduce the interfacial resistance between nanofiller and polymer matrix should be further explored. Recently, as remarkable progress has been made on the electrical conductivity

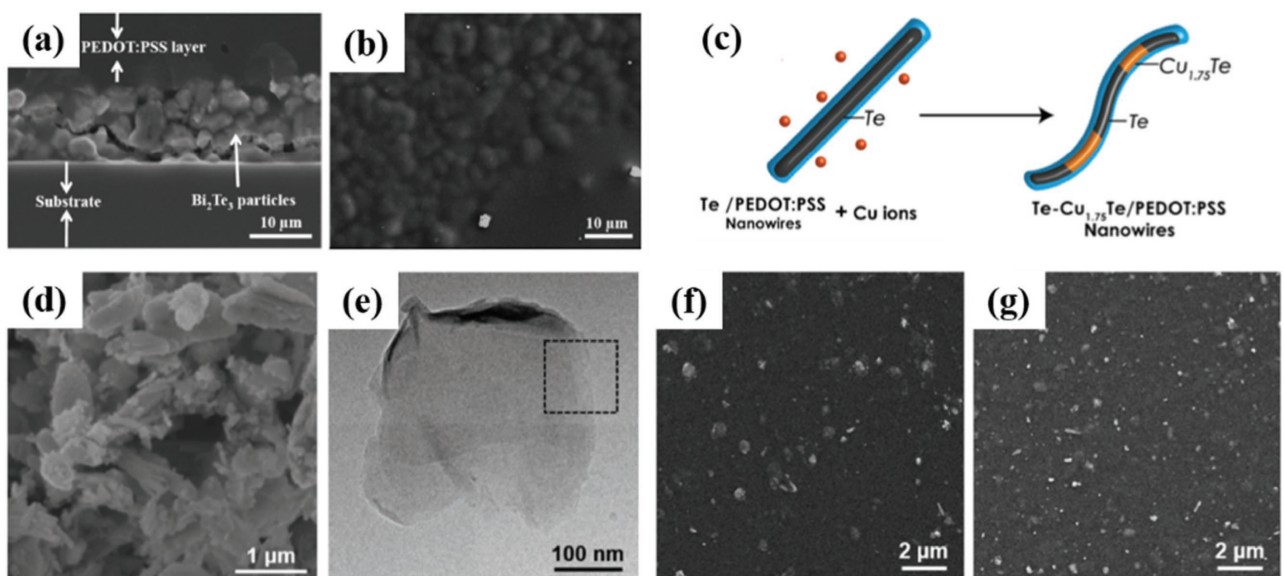


Figure 10. a) Cross-section and b) top-view SEM images of the PH1000 mixed Bi₂Te₃ ball milled particles. c) Schematic diagram of Cu incorporation and nucleation of alloy phases within PEDOT:PSS-Te NWs. d) FE-SEM and e) low-magnification FE-TEM images of the exfoliated SnSe NSs. FE-SEM images for SnSe NS/PEDOT:PSS composites with SnSe content of f) 20% and g) 50 wt%, respectively. Reproduced with permission.^[139,142,148] Copyright 2010, The American Chemical Society.

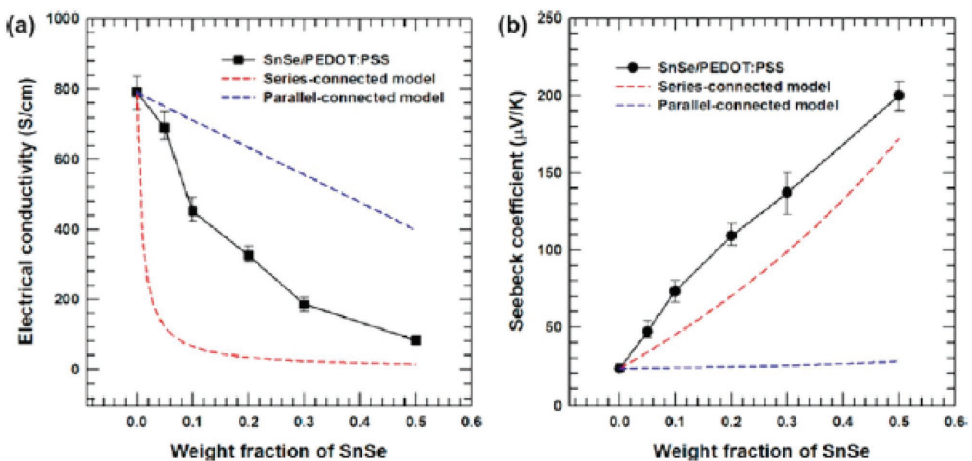


Figure 11. a) Electrical conductivity and b) Seebeck coefficient of the SnSe nanosheet/PEDOT:PSS composites with two models (series- and parallel-connected models) as a function of the SnSe NS concentration. Reproduced with permission.^[142] Copyright 2016, The American Chemical Society.

enhancement of conducting polymers,^[37,149,150] the electrical conductivity of many inorganic/PEDOT composites can be significantly enhanced by posttreatment. Cho et al. treated the as-prepared Te/PEDOT:PSS films with H₂SO₄.^[42] The electrical conductivity is enhanced from 11 to 335 S cm⁻¹, while the Seebeck coefficient decreases from 250 only to 100 μ V K⁻¹. The optimal PF increases to 284 μ W m⁻¹ K⁻² accordingly.

n-type composites were investigated as well. Liang et al. demonstrated high-performance n-type TE composites with Ni NWs dispersed in PVDF.^[151] At a Ni NW loading of 80 wt%, the composites can exhibit an electrical conductivity of 4701 S cm⁻¹ and Seebeck coefficient of -20 μ V K⁻¹, resulting in a PF of 200 μ W m⁻¹ K⁻² at room temperature. This PF value is among the highest for n-type TE composites.

4.2. Polymer Composites with Carbon Nanomaterials

Besides conventional inorganic TE materials, nanostructured carbon allotropes such as CNTs and graphene are also used as fillers for TE composites.^[152-155] The TE properties of some polymer composites with carbon nanomaterials are listed in Table 7. CNTs and graphene can have high electrical conductivity and thus increase the electrical conductivity of the composites. Similar to the inorganic/organic TE composites, the carbon-based TE composites have also shown decoupled Seebeck coefficient and electrical conductivity and thus promising TE performance. The large specific surface area and conjugated π - π structure of carbon-based nanomaterials also facilitate effective interfacial contacts between the carbon fillers and the conducting polymer matrix, which favorably magnifies the interfacial effects arising from the filler-matrix boundaries. In the meanwhile, the thermal conductivity of the composites still remains low due to the phonon scattering. Such synergistic effect between carbon materials and conducting polymers commonly leads to great TE performance, making carbon/polymer composites more and more popular.

CNTs are popular nanofillers of TE composites. In 2010, Yu et al. reported CNT/PEDOT:PSS TE composites by incorporating CNTs into the insulating gum Arabic (GA) matrix.^[156]

The dispersion of CNTs was aided by the DMSO-added PEDOT:PSS as a surfactant. With well-percolated conducting networks of 35 wt% PEDOT:PSS-coated CNTs, the composites can yield high electrical conductivities of up to 400 S cm⁻¹, while the Seebeck coefficient (\approx 25 μ V K⁻¹) and the thermal conductivity (0.2–0.4 W m⁻¹ K⁻¹) do not remarkably change. As a result, the ZT of the composite is \approx 0.02.^[157] Later, Yu et al. and Grunlan et al. further optimized the composites by using single walled carbon nanotubes (SWCNTs), PEDOT:PSS, and PVAc.^[158-160] The composites consisted of 60 wt% SWCNTs, 30 wt% PEDOT:PSS, and 10 wt% PVAc can have an electrical conductivity of 950 S cm⁻¹. The Seebeck coefficient has a weak dependence on the CNT loading, and its value is \approx 41 μ V K⁻¹. Thus, the composites can show a PF of 160 μ W m⁻¹ K⁻² and ZT of 0.12–0.24. A good modulation of the junctions between CNTs and polymer matrix can be helpful. As shown in Figure 12, the formation of highly electrically connecting but thermally impeding CNT–PEDOT–CNT junctions can provide exceptional TE transport properties for the TE composites.

Posttreatments were also exploited to enhance the electrical conductivity of CNTs/PEDOT:PSS composites. Cho et al. treated double walled CNT (DWCNT)/PEDOT:PSS composites with ethylene glycol and observed the enhancement of the electrical conductivity of the composites by at least 1 order of magnitude.^[161] As a result, the PF increases from 21.6 to 151 μ W m⁻¹ K⁻². Yu et al. treated SWCNT/PEDOT:PSS composites with DMSO or formic acid (FA).^[162] Compared with the untreated ones with the same CNT loading of 6.7 wt%, the DMSO- and FA-treated SWNT/PEDOT:PSS composites exhibit PFs of 464 and 407 μ W m⁻¹ K⁻², respectively, corresponding to the enhancement by a factor of over 300. Chemical treatments on the TE composites in general contribute to the conductivity enhancements rather than altering the Seebeck coefficient. Notably, the FA-treated composites show a Seebeck coefficient lower than the untreated and DMSO-treated composites. This is ascribed to the effective removal of PSSH by FA that may lead to closer proximity of CNTs in the composites. As shown in Figure 13a, the large Seebeck coefficient of the SWCNT/PEDOT:PSS composites originally came from the CNT–PEDOT:PSS–CNT junctions due to the energy filtering effect.



Table 7. Summary of the TE properties of some typical carbon-based fillers/conducting polymer TE composites.

Polymers	Fillers	Synthesis method	Loading [wt%]	$S [\mu\text{V K}^{-1}]$	$\sigma [\text{S cm}^{-1}]$	$\text{PF} [\mu\text{W m}^{-1} \text{K}^{-2}]$	$\kappa [\text{W m}^{-1} \text{K}^{-1}]$	ZT	Ref.
PEDOT:PSS + PVAc	SWNTs	Solution mixing	60	41	950	160	0.2–0.4 ^{a)}	–	[158]
PEDOT:PSS	SWNTs	Liquid exfoliation	85	≈20	≈3300	≈140	0.45–0.69 ^{a)}	≈0.03	[160]
PEDOT:PSS	DWNTs	Solution mixing then EG treatment	20	43.7	780	151	–	–	[161]
PEDOT:PSS	SWNTs	Solution mixing then DMSO treatment	6.7	59	≈1350	464	–	–	[162]
PEDOT:PSS	SWNTs	In situ polymerization	15	≈16.5	329	9	–	–	[165]
PEDOT:PSS	SWNTs	In situ polymerization		≈18	570.4	19	–	–	[165]
PEDOT:PSS	rGO	In situ polymerization	16	31.8	50.8	5.2	–	–	[163]
PEDOT:PSS	rGO	Solution mixing	3	≈17	≈1160	32.6	0.3 ^{b)}	0.03	[175]
PEDOT:PSS	Graphene nanoplatelet	In situ polymerization	3	26.8	637	45.7	–	–	[172]
PEDOT:PSS	Liquid exfoliated graphene	Solution mixing then hydrazine treatment	3	22	1283.5	53.3	0.3	0.05	[173]
PEDOT:PSS	RTCVD graphene	In situ polymerization	Heterostructure	28.1	1096	57.9	–	–	[193]
PANI	MWNTs	In situ polymerization	85	28.6	61.47	5	≈0.45	–	[167]
PANI	SWNTs	In situ polymerization	41.4	40	125	20	1.5 ^{a)}	0.004	[168]
PANI	SWNTs	Solution mixing		65	769	176	0.43 ^{a)}	0.12	[169]
PANI	DWNTs	Solution mixing	30	≈61	610	220	0.7 ^{b)}	≈0.1	[171]
PANI	SWNTs	In situ polymerization then solution mixing	65	38.9	1440	217	0.44 ^{a)}	–	[170]
PANI	Graphene	In situ polymerization then solution mixing	48	26	814	55	–	–	[174]
PPy	SWNTs	In situ polymerization	60	22.2	399	19.7	–	–	[164]
P3HT	SWNTs	In situ polymerization then postdoping	60	31.1	2760	267	–	–	[194]
PPy	rGO	In situ polymerization	50	33.8	75.1	8.56	–	–	[166]

^{a)}Measured thermal conductivity; ^{b)}Calculated thermal conductivity.

After the FA treatment (Figure 13b), the closer proximity or even direct contact of the CNTs in the composites may partially eliminate the effective interfaces and vanish the filtering effect, thereby slightly reducing the Seebeck coefficient.^[158] However, these posttreatment methods still greatly enhanced the overall PF.

In addition to simply mixing the carbon nanofillers and solution-processable polymers for preparing TE composites,

attempts have also been made to prepare composites by synthesizing conducting polymers at the presence of carbon nanofillers. Due to the strong $\pi-\pi$ interaction presented between the carbon lattice and conjugated polymer backbone, such synthesis is also known as “template-directed in situ polymerization.” Chen et al. carried out a series of studies on the direct synthesis of carbon-based TE composites by in situ polymerization of monomers, such as EDOT,^[163] pyrrole,^[164] and aniline. Various shapes, such as pie-like,^[163] cable-like,^[165] and coral-like structures,^[165] were synthesized (Figure 14). Their results indicate that the carbon nanofillers, the thickness of surface coating layers as well as the nanostructures of the conducting polymers can affect the TE performance of the composites. SWCNTs and DWCNTs seem to be superior over MWCNTs due to fewer structural defects, higher specific surface areas and better electrical property.^[152] Chen et al. investigated the thickness effect of the polymer layers coated on the reduced graphene oxide (rGO) surfaces on the Seebeck coefficient and electrical conductivity of rGO/PPy composites.^[166] By adjusting the mass ratios of rGO:PPy from 1:2 to 2:1, the thickness of the surface wrapping layers decreased from 40 to 20 nm accordingly. The Seebeck coefficient and electrical conductivity increase from $21.8 \mu\text{V K}^{-1}$ and 29.4 S cm^{-1} to $26.9 \mu\text{V K}^{-1}$ and 41.6 S cm^{-1} , respectively, with the decrease of the polymer coating thickness.

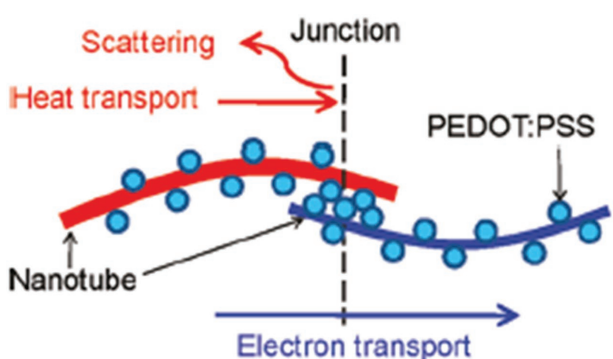
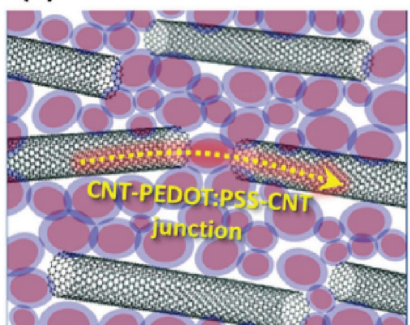


Figure 12. CNT-PEDOT:PSS-CNT junctions made by PEDOT:PSS coating on CNTs. Reproduced with permission.^[158] Copyright 2011, The American Chemical Society.



(a) Low CNT %



(b) High CNT %

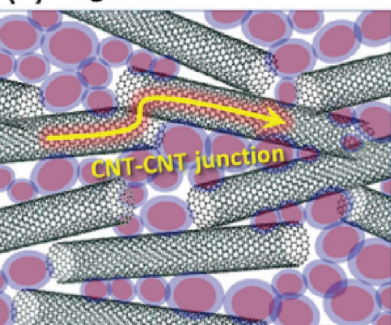


Figure 13. Schematic structure and charge transport of the CNT/PEDOT:PSS composites at a) low and b) high CNT concentrations. Reproduced with permission.^[162] Copyright 2017, Elsevier.

Apart from the contribution of the intrinsic electrical conductivity and Seebeck coefficient to the TE properties of composites, carbon nanofillers can help align the polymer chains and thus increase the TE properties of carbon/conducting polymer composites. MWCNT/PANI and SWCNT/PANI composites were prepared via an *in situ* polymerization process.^[167,168] Both the composites exhibited higher Seebeck coefficients and PFs than neat PANI. The former exhibits a PF of $5 \mu\text{W m}^{-1} \text{K}^{-2}$,^[167] while the latter shows a PF of $20 \mu\text{W m}^{-1} \text{K}^{-2}$. Apart from the higher conductivity of SWCNTs than MWCNTs, SWCNTs can cause the PANI chains to align in a more ordered manner as revealed by SEM, XRD, and Raman spectra (Figure 15).^[168] Later, Chen et al. and Yu et al. further modified the preparation process by doping PANI with camphorsulfonic acid (CSA) or *m*-cresol.^[169–171] The crystallinity of the PANI molecules and the carrier mobility were further improved. At 64 wt% SWNT loading, the composites can have an electrical conductivity of 769 S cm^{-1} and Seebeck coefficient of $65 \mu\text{V K}^{-1}$. The corresponding PF reaches $\approx 220 \mu\text{W m}^{-1} \text{K}^{-2}$.

Graphene is also a popular nanofiller of TE composites.^[132] Kim et al. reported the *in situ* synthesis of PEDOT:PSS at the presence of graphene nanoplatelets.^[172] At a graphene loading of 3 wt%, they observed a PF of $45.7 \mu\text{W m}^{-1} \text{K}^{-2}$, higher than that ($24.2 \mu\text{W m}^{-1} \text{K}^{-2}$) of neat PEDOT:PSS. Xu et al. incorporated the liquid-exfoliated graphene into commercial PEDOT:PSS and obtained a PF of $53.5 \mu\text{W m}^{-1} \text{K}^{-2}$ at the graphene loading of 3 wt%.^[173] Graphene/PANI composites were also been prepared.^[174] At the optimal graphene loading of 48 wt%,

the composites can exhibit an electrical conductivity of 814 S cm^{-1} , Seebeck coefficient of $26 \mu\text{V K}^{-1}$, and PF of $55 \mu\text{W m}^{-1} \text{K}^{-2}$. There are a couple of different approaches to prepare graphene, such as mechanically exfoliation, CVD growth and chemically reduction of graphene oxide. The preparation approach affects the TE properties of the composites.^[173,175–177]

4.3. Polymer Composites with Nanostructured Polymers as the Fillers

Nanostructured polymers were also investigated as the nanofillers of TE composites. The TE properties of some composites are shown in Table 8. The polymeric nature of both the fillers and matrix ensures low thermal conductivity of the composites. All PEDOT-based TE composites were prepared by integrating PEDOT nanowires into PEDOT:Tos matrix.^[68,178] At the loading of 0.2 wt% PEDOT nanowires, the composites can show a Seebeck coefficient of $59.3 \mu\text{V K}^{-1}$, electrical conductivity of 1270 S cm^{-1} , and PF of $446.6 \mu\text{W m}^{-1} \text{K}^{-2}$. Such a high PF is also ascribed to the interfacial energy filtering effect arising from the interface between the PEDOT nanowires and PEDOT:Tos. Zhang et al. investigated the role of carrier scattering in all polymer TE composites through experiments and simulation.^[179] They concluded that the TE enhancement by the interfacial scattering could be significant only if the carrier mobility of the polymer matrix is higher than $1 \text{ cm}^2 \text{ V}^{-1} \text{s}^{-1}$. They observed a ZT of 0.44.

Apart from composites with nanofillers, composites with multiple layers of polymers can also exhibit high TE performance. Jo et al. prepare composites with alternative PEDOT:PSS and PANI-CSA layers via layer-by-layer (LBL) deposition^[180] (Figure 16). The electrical conductivity and PF of a composite of 5 PEDOT:PSS/PANI-CSA layers are 1.3 and 2 times as those of neat PEDOT:PSS, respectively. They attributed the high PF to the stretched PEDOT and PANI chains and the hole diffusion from PANI-CSA to PEDOT:PSS arising from such multilayered structure

Highly stretchable elastomers like waterborne polyurethane (WPU) and poly(dimethylsiloxane) were as adopted as the matrix of conducting polymer fillers.^[181] The high stretchability

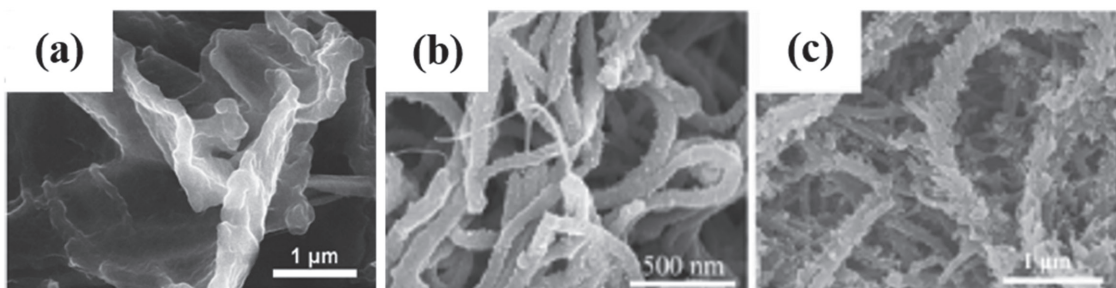


Figure 14. SEM images of CNT/PEDOT TE composites with a) pie-like, b) cable-like, and c) coral-like structure. Reproduced with permission.^[163,165] Copyright 2013, Royal Society of Chemistry. Copyright 2017, Elsevier.

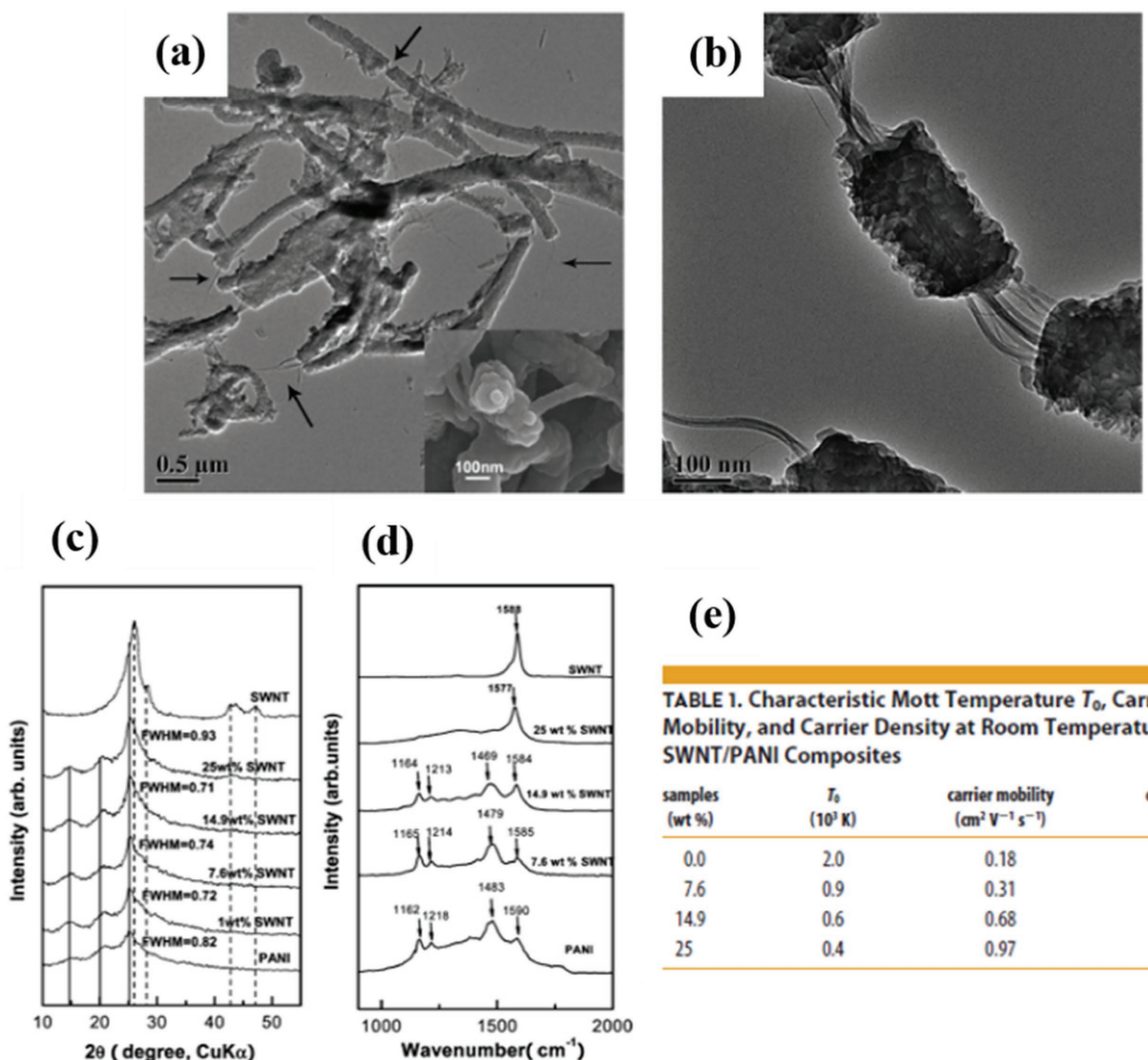


Figure 15. a,b) TEM images of SWNT/PANI composites. c) XRD patterns and d) Raman spectra of SWNT/PANI composites with different SWNT contents. e) Carrier transport characteristics of SWNT/PANI composites. Reproduced with permission.^[168] Copyright 2010, The American Chemical Society.

can give the composites potential application in wearable electronics. A PF of $11 \mu\text{W m}^{-1} \text{K}^{-2}$ was reported.^[182–184]

4.4. Composites with Three or More Components

To make use of the synergetic effects of different fillers or rational design of the interfaces, TE composites with three or more components were investigated. The TE properties are summarized

in Table 9. Kim et al. synthesized PEDOT:PSS in the presence of graphene and CNTs.^[185] They found that PEDOT:PSS, graphene and MWCNTs could have synergetic effects and the TE properties were superior over any individual component or composites of any two components. The PEDOT:PSS/graphene/CNT composites can exhibit a PF of $37.08 \mu\text{W m}^{-1} \text{K}^{-2}$ and ZT of 0.031. The TE enhancement was attributed to the electronic coupling between PEDOT and the two carbon nanomaterials. The TE properties of Te/PDODT:PSS composites were greatly improved

Table 8. Summary of the TE properties for some typical polymer/polymer TE composites.

Polymers	Fillers	Synthesis method	$S [\mu\text{V K}^{-1}]$	$\sigma [\text{S cm}^{-1}]$	$\text{PF} [\mu\text{W m}^{-1} \text{K}^{-2}]$	$\kappa [\text{W m}^{-1} \text{K}^{-1}]$	ZT	Ref.
PEDOT:Tos	PEDOT nanowires	In situ polymerization	59.3	1270	446.6	0.286 ^{a)}	0.44	[68]
PEDOT/PANI		LBL deposition	17.5	1585	49	0.24 ^{b)}	–	[180]
WPU	PEDOT:PSS + MWNTs	Solution mixing	10	138.26	1.41	–	–	[181]

^{a)}Measured thermal conductivity; ^{b)}Calculated thermal conductivity.

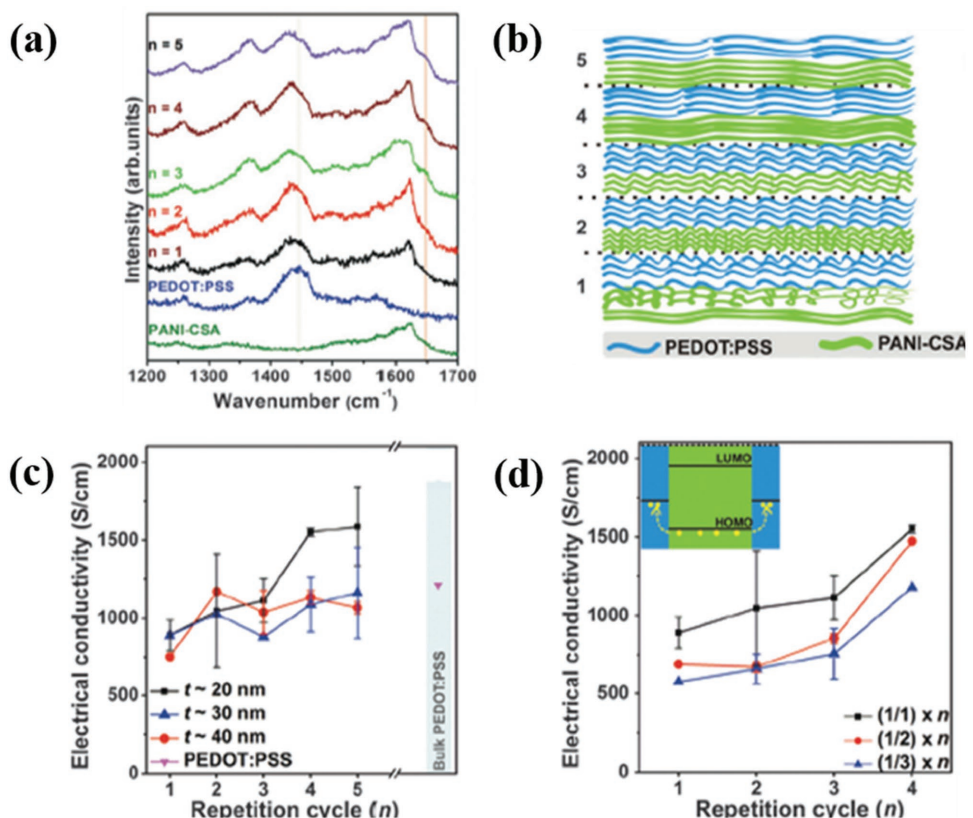


Figure 16. a) Raman spectra of PEDOT:PSS, PANi-CSA, and multilayer film. b) Schematic diagram explaining the stretching of chain of both the PEDOT:PSS and PANi-CSA layer. c) Electrical conductivity and d) layer thickness ratio-dependent as a function of the repetition cycle. Reproduced with permission.^[180] Copyright 2016, The Royal Society of Chemistry.

by the addition of a small amount of nanocarbons such as graphene^[186] or SWCNTs.^[187] At a loading of 0.3 wt% SWNT, the SWCNT/Te/PEDOT:PSS composites can have a PF of $206 \mu\text{W m}^{-1} \text{K}^{-2}$ with an electrical conductivity of 139 S cm^{-1} and Seebeck coefficient of $118 \mu\text{V K}^{-1}$.^[187]

Grunlan et al. prepared composites with multiple layers of PANi/graphene-PEDOT:PSS/PANI/DWCNT-PEDOT:PSS via LBL deposition.^[188–191] PEDOT:PSS was used as a surfactant to stabilize graphene and DWCNTs in the dispersions. The composites can exhibit an electrical conductivity of 1900 S cm^{-1} ,

Seebeck coefficient of $120 \mu\text{V K}^{-1}$ and a PF of $2710 \mu\text{W m}^{-1} \text{K}^{-2}$. The PF is comparable to that of the best inorganic TE materials like Bi_2Te_3 at room temperature.^[189] But the graphene and DWCNTs can lead to significantly high thermal conductivity.

n-type multilayered composites with good air stability were also prepared by the LBL technique.^[190] A composite film consisting of 80 bilayered DWCNT-polyethyleneimine (PEI)/graphene-polyvinylpyrrolidone (PVP) can show an electrical conductivity of 300 S cm^{-1} , Seebeck coefficient of $-80 \mu\text{V K}^{-1}$ and PF of $190 \mu\text{W m}^{-1} \text{K}^{-2}$ at room temperature.

Table 9. Summary of the TE properties for some typical multicomponent TE composites.

Polymers	Fillers	Synthesis method	Loading [wt%]	$S [\mu\text{V K}^{-1}]$	$\sigma [\text{S cm}^{-1}]$	$\text{PF} [\mu\text{W m}^{-1} \text{K}^{-2}]$	$\kappa [\text{W m}^{-1} \text{K}^{-1}]$	ZT	Ref.
PEDOT:PSS	Te–Cu _{1.75} Te	In situ synthesis	57	220	17.4	84	–	–	[148]
PEDOT:PSS	MWNT + rGO	In situ polymerization	5	23.2	689	37.08	$0.36^{\text{a})}$	0.031	[185]
PANI	DWNTs + Graphene	LBL deposition	62.3	130	1080	1825	$0.3\text{--}10^{\text{b})}$	0.05–1.8	[188]
PEDOT:PSS	Te + rGO	In situ polymerization then solution mixing	≈ 17	202	35	143	$0.21^{\text{a})}$	≈ 0.21	[186]
PEDOT:PSS	Te + SWNTs	In situ polymerization then solution mixing	0.3	118	139	206	–	–	[187]
PANI / PEDOT:PSS	DWNTs + Graphene	LBL deposition	54.3	120	1900	2710	$0.4\text{--}24.6^{\text{b})}$	0.03–2	[189]
PEI/PVP	DWNT + graphene	LBL deposition	88.8	–80	300	190	$0.1\text{--}20^{\text{b})}$	0.002–0.56	[190]
PANI	SWNTs + Au NPs	Vacuum infiltration	–	150.86	1106	2454	$3.61^{\text{a})}$	0.203	[192]

^{a)}Measured thermal conductivity; ^{b)}Calculated thermal conductivity.



To enhance the electrical conductivity, attempts have also been made to add gold nanoparticles into some binary TE composites.^[192] An et al. fabricated gold-doped CNT/PANI networks and observed a PF of 2454 $\mu\text{W m}^{-1}\text{ K}^{-2}$ at room temperature.^[192] However, the high CNT loading and the Au decoration caused the thermal conductivity of the composites to be 3.61 $\text{W m}^{-1}\text{ K}^{-1}$. The corresponding ZT was thus 0.203 at room temperature.

5. Outlook and Summary

Polymer and polymer-based composite are promising TE materials for thermoelectric devices. So far, the polythiophene derivatives including PEDOT as p-type polymers have attracted the most attention due to their high PF values up to hundreds of $\mu\text{W m}^{-1}\text{ K}^{-2}$ at room temperature. In order to acquire high conductivity, the polythiophene derivatives should possess some features such as high carrier mobility, well-ordered structure, good surface morphology and high doping level. Thus the selection of polymers, effective dopant and appropriate doping process are very important. However, the effect of polymer chemical structure or molecular ordering on the Seebeck coefficient is still unclear. Therefore, the structure–property relationship and doping engineering need to be studied further in future.

Unlike the p-type counterparts, the n-type polymers typically suffer from a low conductivity and poor air-stability. Among them, polymers with coordinate bonds like Ni–S can have good stability and high thermoelectric properties. In order to gain good understanding on the relationship between thermoelectric properties and chemical structure, more metal-containing polymers should be synthesized and studied. In addition, posttreatment approaches to optimize the morphology and the doping level of these metal-containing polymers should be developed.

Inorganic TE materials and carbon nanomaterials have been used as fillers of conducting polymers. These composites can exhibit high thermoelectric properties arising from the synergistic effects of the components. It has been observed that the thermal conductivity of these composites can be comparable to the polymers due to the phonon scattering effect when the filler loading is not too high.

Although great progress has been made in TE polymers and composites, there is still much room for the further improvement. It is highly possible that the ZT value of TE polymers can be comparable to or even better than that of the best inorganic TE materials. Polymers and composites with high ZT values will enable the fabrication of flexible TE systems including TE generators and Peltier coolers. These flexible TE systems will have important application in many areas, such as harvesting of low-grade heat and wearable electronics.

Acknowledgements

This work was financially supported by the Ministry of Education, Singapore (R-284-000-156-112), the Natural Science Foundation of China (61504015), the Natural Science Foundation of Chongqing (cstc2017jcyjAX0451), the Key Laboratory of Low-grade Energy Utilization Technologies and Systems (LLEUTS-2017004), and Fundamental Research Funds for the Central Universities (106112017CDJQJ148805).

Conflict of Interest

The authors declare no conflict of interest.

Keywords

conductivity, power factor, Seebeck coefficient, thermoelectric composites, thermoelectric polymers

Received: October 26, 2017

Revised: December 7, 2017

Published online: January 22, 2018

- [1] Y. Chen, Y. Zhao, Z. Liang, *Energy Environ. Sci.* **2015**, *8*, 401.
- [2] L. E. Bell, *Science* **2008**, *321*, 1457.
- [3] T. M. Tritt, M. A. Subramanian, *MRS Bull.* **2006**, *31*, 188.
- [4] G. J. Snyder, E. S. Toberer, *Nat. Mater.* **2008**, *7*, 105.
- [5] Q. Zhang, Y. Sun, W. Xu, D. Zhu, *Adv. Mater.* **2014**, *26*, 6829.
- [6] B. Russ, A. Glaudell, J. J. Urban, M. L. Chabinyc, R. A. Segalman, *Nat. Rev. Mater.* **2016**, *1*, 16050.
- [7] O. Bubnova, X. Crispin, *Energy Environ. Sci.* **2012**, *5*, 9345.
- [8] J. Yang, H. L. Yip, A. K.-Y. Jen, *Adv. Energy Mater.* **2013**, *3*, 549.
- [9] S. Kirchmeyer, K. Reuter, *J. Mater. Chem.* **2005**, *15*, 2077.
- [10] A. Elschner, S. Kirchmeyer, W. Lovenich, U. Merker, K. Reuter, *PEDOT: Principles and Application of an Intrinsically Conductive Polymer*, CRC Press, Boca Raton, FL, USA **2010**.
- [11] Y. Xia, J. Ouyang, *ACS Appl. Mater. Interfaces* **2012**, *4*, 4131.
- [12] J. Ouyang, *ACS Appl. Mater. Interfaces* **2013**, *5*, 13082.
- [13] J. Luo, D. Billep, T. Blaudeck, E. Sheremet, R. D. Rodriguez, D. R. Zahn, M. Toader, M. Hietschold, T. Otto, T. Gessner, *J. Appl. Phys.* **2014**, *115*, 054908.
- [14] J. Xiong, F. Jiang, W. Zhou, C. Liu, J. Xu, *RSC Adv.* **2015**, *5*, 60708.
- [15] S. Liu, H. Deng, Y. Zhao, S. Ren, Q. Fu, *RSC Adv.* **2015**, *5*, 1910.
- [16] L. Zhang, H. Deng, S. Liu, Q. Zhang, F. Chen, Q. Fu, *RSC Adv.* **2015**, *5*, 105592.
- [17] S. Zhang, Z. Yu, P. Li, B. Li, F. H. Isikgor, D. Du, K. Sun, Y. Xia, J. Ouyang, *Org. Electron.* **2016**, *32*, 149.
- [18] Y. Xia, J. Fang, P. Li, B. Zhang, H. Yao, J. Chen, J. Ding, J. Ouyang, *ACS Appl. Mater. Interfaces* **2017**, *9*, 19001.
- [19] J. Y. Kim, J. H. Jung, D. E. Lee, J. Joo, *Synth. Met.* **2002**, *126*, 311.
- [20] J. Ouyang, Q. Xu, C. Chu, Y. Yang, G. Li, J. Shinar, *Polymer* **2004**, *45*, 8443.
- [21] J. Ouyang, C. Chu, F. Chen, Q. Xu, Y. Yang, *Adv. Funct. Mater.* **2005**, *15*, 203.
- [22] J. Ouyang, Y. Yang, *Adv. Mater.* **2006**, *18*, 2141.
- [23] F. X. Jang, J. K. Xing, B. Y. Lu, Y. Xie, R. J. Huang, L. F. Li, *Chin. Phys. Lett.* **2008**, *25*, 2202.
- [24] B. Fan, X. Mei, J. Ouyang, *Macromolecules* **2008**, *41*, 5971.
- [25] C. Liu, B. Lu, J. Yan, J. Xu, R. Yue, Z. Zhu, S. Zhou, X. Hu, Z. Zhang, P. Chen, *Synth. Met.* **2010**, *160*, 2481.
- [26] F. F. Kong, C. C. Liu, J. K. Xu, F. X. Jiang, B. Y. Lu, R. R. Yue, G. D. Liu, J. M. Wang, *Chin. Phys. Lett.* **2011**, *28*, 037201.
- [27] F. Kong, C. Liu, H. Song, J. Xu, Y. Huang, H. Zhu, J. Wang, *Synth. Met.* **2013**, *185*, 31.
- [28] J. Ouyang, *Displays* **2013**, *34*, 423.
- [29] C. Yi, A. Wilhite, L. Zhang, R. Hu, S. S. Chuang, J. Zheng, X. Gong, *ACS Appl. Mater. Interfaces* **2015**, *7*, 8984.
- [30] Y. Xia, J. Ouyang, *Macromolecules* **2009**, *42*, 4141.
- [31] Y. Xia, J. Ouyang, *ACS Appl. Mater. Interfaces* **2010**, *2*, 474.
- [32] Y. Xia, J. Ouyang, *Org. Electron.* **2010**, *11*, 1129.
- [33] Y. Xia, H. Zhang, J. Ouyang, *J. Mater. Chem.* **2010**, *20*, 9740.
- [34] Y. Xia, J. Ouyang, *J. Mater. Chem.* **2011**, *21*, 4927.



- [35] K. Sun, Y. Xia, J. Ouyang, *Sol. Energy Mater. Sol. Cells* **2012**, *97*, 89.
- [36] Y. Xia, J. Ouyang, *Org. Electron.* **2012**, *13*, 1785.
- [37] D. A. Mengistie, C. H. Chen, K. M. Boopathi, F. W. Pranoto, L. J. Li, C. W. Chu, *ACS Appl. Mater. Interfaces* **2014**, *7*, 94.
- [38] K. Sun, S. Zhang, P. Li, Y. Xia, X. Zhang, D. Du, F. H. Isikgor, J. Ouyang, *J. Mater. Sci.: Mater. Electron.* **2015**, *26*, 4438.
- [39] Y. Xia, K. Sun, J. Chang, J. Ouyang, *J. Mater. Chem. A* **2015**, *3*, 15897.
- [40] H. Shi, C. Liu, Q. Jiang, J. Xu, *Adv. Electron. Mater.* **2015**, *1*, 1500017.
- [41] Z. Yu, Y. Xia, D. Du, J. Ouyang, *ACS Appl. Mater. Interfaces* **2016**, *8*, 11629.
- [42] E. J. Bae, Y. H. Kang, K. S. Jang, S. Y. Cho, *Sci. Rep.* **2016**, *6*, 18805.
- [43] Z. Fan, D. Du, Z. Yu, P. Li, Y. Xia, J. Ouyang, *ACS Appl. Mater. Interfaces* **2016**, *8*, 23204.
- [44] S. Zhang, Y. Xia, J. Ouyang, *Org. Electron.* **2017**, *45*, 139.
- [45] F. Wu, P. Li, K. Sun, Y. Zhou, W. Chen, J. Fu, M. Li, S. Lu, D. Wei, X. Tang, Z. Zang, L. Sun, X. Liu, J. Ouyang, *Adv. Electron. Mater.* **2017**, *3*, 1700047.
- [46] O. Bubnova, Z. U. Khan, H. Wang, S. Braun, D. R. Evans, M. Fabretto, P. Hojati-Talemi, D. Dagnelund, J.-B. Arlin, S. D. Yves, H. Geerts, D. W. Breiby, J. W. Andreasen, R. Lazzaroni, W. M. Chen, I. Zozoulenko, M. Fahlman, P. J. Murphy, M. Berggren, X. Crispin, *Nat. Mater.* **2014**, *13*, 190.
- [47] O. Bubnova, M. Berggren, X. Crispin, *J. Am. Chem. Soc.* **2012**, *134*, 16456.
- [48] T.-C. Tsai, H.-C. Chang, C.-H. Chen, W.-T. Whang, *Org. Electron.* **2011**, *12*, 2159.
- [49] J. Luo, D. Billep, T. Waechtler, T. Otto, M. Toader, O. Gordan, E. Sheremet, J. Martin, M. Hietschold, D. R. Zahn, T. Gessner, *J. Mater. Chem. A* **2013**, *1*, 7576.
- [50] S. H. Lee, H. Park, W. Son, H. H. Choi, J. H. Kim, *J. Mater. Chem. A* **2014**, *2*, 13380.
- [51] N. Massonnet, A. Carella, O. Jaudouin, P. Rannou, G. Laval, C. Celle, J.-P. Simonato, *J. Mater. Chem. C* **2014**, *2*, 1278.
- [52] T.-C. Tsai, H.-C. Chang, C.-H. Chen, Y.-C. Huang, W.-T. Whang, *Org. Electron.* **2014**, *15*, 641.
- [53] H. Park, S. H. Lee, F. S. Kim, H. H. Choi, I. W. Cheong, J. H. Kim, *J. Mater. Chem. A* **2014**, *2*, 6532.
- [54] S. H. Lee, H. Park, S. Kim, W. Son, I. W. Cheong, J. H. Kim, *J. Mater. Chem. A* **2014**, *2*, 7288.
- [55] Z. Fan, D. Du, H. Yao, J. Ouyang, *ACS Appl. Mater. Interfaces* **2017**, *9*, 11732.
- [56] Z. Fan, P. Li, D. Du, J. Ouyang, *Adv. Energy Mater.* **2017**, *7*, 1602116.
- [57] M. Culebras, C. M. Gomez, A. Cantarero, *J. Mater. Chem. A* **2014**, *2*, 10109.
- [58] I. Petsagkourakis, E. Pavlopoulou, G. Portale, B. A. Kuropatwa, S. Dilhaire, G. Fleury, G. Hadzioannou, *Sci. Rep.* **2016**, *6*, 30501.
- [59] C. Yi, L. Zhang, R. Hu, S. S. Chuang, J. Zheng, X. Gong, *J. Mater. Chem. A* **2016**, *4*, 12730.
- [60] Y. H. Lee, J. Oh, S. S. Lee, H. Kim, J. G. Son, *ACS Macro Lett.* **2017**, *6*, 386.
- [61] T. Park, C. Park, B. Kim, H. Shin, E. Kim, *Energ. Environ. Sci.* **2013**, *6*, 788.
- [62] O. Bubnova, Z. U. Khan, A. Malti, S. Braun, M. Fahlman, M. Berggren, X. Crispin, *Nat. Mater.* **2011**, *10*, 429.
- [63] Z. U. Khan, O. Bubnova, M. J. Jafari, R. Brooke, X. Liu, R. Gabrielsson, T. Ederth, D. R. Evans, J. W. Andreasen, M. Fahlman, X. Crispin, *J. Mater. Chem. C* **2015**, *3*, 10616.
- [64] J. Wang, K. Cai, S. Shen, *Org. Electron.* **2015**, *17*, 151.
- [65] J. Wang, K. Cai, H. Song, S. Shen, *Synth. Met.* **2016**, *220*, 585.
- [66] J. Zhao, D. Tan, G. Chen, *J. Mater. Chem. C* **2017**, *5*, 47.
- [67] X. Hu, G. Chen, X. Wang, H. Wang, *J. Mater. Chem. A* **2015**, *3*, 20896.
- [68] K. Zhang, J. Qiu, S. Wang, *Nanoscale* **2016**, *8*, 8033.
- [69] K. Hiraishi, A. Masuhara, H. Nakanishi, H. Oikawa, Y. Shinohara, *Jpn. J. Appl. Phys.* **2009**, *48*, 071501.
- [70] Y. Hu, H. Shi, H. Song, C. Liu, J. Xu, L. Zhang, Q. Jiang, *Synth. Met.* **2013**, *181*, 23.
- [71] J. Sinha, S. J. Lee, H. Kong, T. W. Swift, H. E. Katz, *Macromolecules* **2013**, *46*, 708.
- [72] Q. Zhang, Y. Sun, W. Xu, D. Zhu, *Energy Environ. Sci.* **2012**, *5*, 9639.
- [73] A. M. Glaudell, J. E. Cochra, S. N. Patel, M. L. Chabinyc, *Adv. Energy Mater.* **2015**, *5*, 1401072.
- [74] S. N. Patel, A. M. Glaudell, D. Kiefer, M. L. Chabinyc, *ACS Macro Lett.* **2016**, *5*, 268.
- [75] S. N. Patel, A. M. Glaudell, K. A. Peterson, E. M. Thomas, K. A. O'Hara, E. Lim, M. L. Chabinyc, *Sci. Adv.* **2017**, *3*, e1700434.
- [76] I. H. Jung, C. T. Hong, U. H. Lee, Y. H. Kang, K. S. Jang, S. Y. Cho, *Sci. Rep.* **2017**, *7*, 44704.
- [77] Q. Zhang, Y. Sun, W. Xu, D. Zhu, *Macromolecules* **2014**, *47*, 609.
- [78] H. Li, M. E. DeCoster, R. M. Ireland, J. Song, P. E. Hopkins, H. E. Katz, *J. Am. Chem. Soc.* **2017**, *139*, 11149.
- [79] J. Sun, M. L. Yeh, B. J. Jung, B. Zhang, J. Feser, A. Majumdar, H. E. Katz, *Macromolecules* **2010**, *43*, 2897.
- [80] C. O. Yoon, M. Reghu, D. Moses, Y. Cao, A. J. Heeger, *Synth. Met.* **1995**, *69*, 255.
- [81] E. R. Holland, A. P. Monkman, *Synth. Met.* **1995**, *74*, 75.
- [82] N. Mateeva, H. Niculescu, J. Schlenoff, L. R. Testardi, *J. Appl. Phys.* **1998**, *83*, 3111.
- [83] H. Yan, T. Ohta, N. Toshima, *Macromol. Mater. Eng.* **2001**, *286*, 139.
- [84] Y. Sun, Z. Wei, W. Xu, D. Zhu, *Synth. Met.* **2010**, *160*, 2371.
- [85] J. Wu, Y. Sun, W. Xu, Q. Zhang, *Synth. Met.* **2014**, *189*, 177.
- [86] Y. Hiroshige, M. Ookawa, N. Toshima, *Synth. Met.* **2006**, *156*, 1341.
- [87] Y. Hiroshige, M. Ookawa, N. Toshima, *Synth. Met.* **2007**, *157*, 467.
- [88] J. Wu, Y. Sun, W. B. Pei, L. Huang, W. Xu, Q. Zhang, *Synth. Met.* **2014**, *196*, 173.
- [89] L. Liang, G. Chen, C. Y. Guo, *Mater. Chem. Front.* **2017**, *1*, 380.
- [90] N. Dubey, M. Leclerc, *J. Polym. Sci., Part B: Polym. Phys.* **2011**, *49*, 467.
- [91] S. Wakim, B. R. Aich, Y. Tao, M. Leclerc, *Polym. Rev.* **2008**, *48*, 432.
- [92] B. R. Aich, N. Blouin, A. Bouchard, M. Leclerc, *Chem. Mater.* **2009**, *21*, 751.
- [93] L. Wang, C. Pan, A. Liang, X. Zhou, W. Zhou, T. Wan, L. Wang, *Polym. Chem.* **2017**, *8*, 4644.
- [94] Y. Nogami, H. Kaneko, T. Ishiguro, A. Takahashi, J. Tsukamoto, N. Hosoi, *Solid State Commun.* **1990**, *76*, 583.
- [95] A. Nollau, M. Pfeiffer, T. Fritz, K. Leo, *J. Appl. Phys.* **2000**, *87*, 4340.
- [96] J. L. Banal, J. Subbiah, H. Graham, J.-K. Lee, K. P. Ghiggino, W. W. H. Wong, *Polym. Chem.* **2013**, *4*, 1077.
- [97] R. Schmidt, J. H. Oh, Y.-S. Sun, M. Deppisch, A.-M. Krause, K. Radacki, H. Braunschweig, M. Könenmann, P. Erk, Z. Bao, F. Würthner, *J. Am. Chem. Soc.* **2009**, *131*, 6215.
- [98] Y. Fukutomi, M. Nakano, J. Y. Hu, I. Osaka, K. Takimiya, *J. Am. Chem. Soc.* **2013**, *135*, 11445.
- [99] T. Menke, D. Ray, J. Meiss, K. Leo, M. Riede, *Appl. Phys. Lett.* **2012**, *100*, 093304.
- [100] P. Wei, J. H. Oh, G. Dong, Z. Bao, *J. Am. Chem. Soc.* **2010**, *132*, 8852.
- [101] C. D. Weber, C. Bradley, M. C. Lonergan, *J. Mater. Chem. A* **2014**, *2*, 303.
- [102] J. Lu, S. Nagase, D. Yu, H. Ye, R. Han, Z. Gao, S. Zhang, L. Peng, *Phys. Rev. Lett.* **2004**, *93*, 116804.
- [103] G. Kim, A. R. Han, H. R. Lee, J. Lee, J. H. Oh, C. Yang, *Chem. Commun.* **2014**, *50*, 2180.
- [104] M. Nakano, I. Osaka, K. Takimiya, *Macromolecules* **2015**, *48*, 576.
- [105] B. D. Naab, X. Gu, T. Kurosawa, J. W. F. To, A. Salleo, Z. Bao, *Adv. Electron. Mater.* **2016**, *2*, 1600004.
- [106] D. Moses, J. Chen, A. Denenstein, M. Kaveh, T. C. Chung, A. J. Heeger, A. G. MacDiarmid, Y. W. Park, *Solid State Commun.* **1981**, *40*, 1007.



- [107] T. Lei, J. H. Dou, X. Y. Cao, J. Y. Wang, J. Pei, *J. Am. Chem. Soc.* **2013**, *135*, 12168.
- [108] K. Shi, F. Zhang, C. A. Di, T. W. Yan, Y. Zou, X. Zhou, D. Zhu, J. Y. Wang, J. Pei, *J. Am. Chem. Soc.* **2015**, *137*, 6979.
- [109] W. Ma, K. Shi, Y. Wu, Z. Y. Lu, H. Y. Liu, J. Y. Wang, J. Pei, *ACS Appl. Mater. Interfaces* **2016**, *8*, 24737.
- [110] Z. Chen, Y. Zheng, H. Yan, A. Facchetti, *J. Am. Chem. Soc.* **2009**, *131*, 8.
- [111] X. Huang, P. Sheng, Z. Tu, F. Zhang, J. Wang, H. Geng, Y. Zou, C. A. Di, Y. Yi, Y. Sun, W. Xu, D. Zhu, *Nat. Commun.* **2015**, *6*, 7408.
- [112] Y. Sun, P. Sheng, C. Di, F. Jiao, W. Xu, D. Qiu, D. Zhu, *Adv. Mater.* **2012**, *24*, 932.
- [113] Y. Sun, L. Qiu, L. Tang, H. Geng, H. Wang, F. Zhang, D. Huang, W. Xu, P. Yue, Y. S. Guan, F. Jiao, D. Tang, C. A. Di, Y. Yi, D. Zhu, *Adv. Mater.* **2016**, *28*, 3351.
- [114] R. A. Schlitz, F. G. Brunetti, A. M. Glaudell, P. L. Miller, M. A. Brady, C. J. Takacs, C. J. Hawker, M. L. Chabinyc, *Adv. Mater.* **2014**, *26*, 2825.
- [115] Y. Wang, M. Nakano, T. Michinobu, Y. Kiyota, T. Mori, K. Takimiya, *Macromolecules* **2017**, *50*, 857.
- [116] S. Wang, H. Sun, U. Ail, M. Vagin, P. O. Persson, J. W. Andreasen, W. Thiel, M. Berggren, X. Crispin, D. Fazzi, S. Fabiano, *Adv. Mater.* **2016**, *28*, 10764.
- [117] J. Chen, J. Zhang, Y. Zou, W. Xu, D. Zhu, *J. Mater. Chem. A* **2017**, *5*, 9891.
- [118] J. R. Reynolds, J. C. W. Chien, C. P. Lillya, *Macromolecules* **1987**, *20*, 1184.
- [119] J. R. Reynolds, F. E. Karasz, C. P. Lillya, J. C. W. Chien, *J. Chem. Soc., Chem. Commun.* **1985**, 268.
- [120] C. Faulmann, J. Chahine, K. Jacob, Y. Coppel, L. Valade, D. de Caro, *J. Nanopart. Res.* **2013**, *15*, 1586.
- [121] K. Oshima, Y. Shiraishi, N. Toshima, *Chem. Lett.* **2015**, *44*, 1185.
- [122] Y. Sun, J. Zhang, L. Liu, Y. Qin, Y. Sun, W. Xu, D. Zhu, *Sci. China Chem.* **2016**, *59*, 1323.
- [123] L. Liu, Y. Sun, W. Li, J. Zhang, X. Huang, Z. Chen, Y. Sun, C. Di, W. Xu, D. Zhu, *Mater. Chem. Front.* **2017**.
- [124] C. Yu, Y. S. Kim, D. Kim, J. C. Grunlan, *Nano Lett.* **2008**, *8*, 4428.
- [125] C. A. Hewitt, A. B. Kaiser, M. Craps, R. Czerw, S. Roth, D. L. Carroll, *Synth. Met.* **2013**, *165*, 56.
- [126] L.-D. Zhao, S.-H. Lo, Y. Zhang, H. Sun, G. Tan, C. Uher, C. Wolverton, V. P. Dravid, M. G. Kanatzidis, *Nature* **2014**, *508*, 373.
- [127] H. Yang, J.-H. Bahk, T. Day, A. M. S. Mohammed, B. Min, G. J. Snyder, A. Shakouri, Y. Wu, *Nano Lett.* **2014**, *14*, 5398.
- [128] Y. Pei, Z. M. Gibbs, A. Gloskovskii, B. Balke, W. G. Zeier, G. J. Snyder, *Adv. Energy Mater.* **2014**, *4*, 1400486.
- [129] K. C. See, J. P. Feser, C. E. Chen, A. Majumdar, J. J. Urban, R. A. Segalman, *Nano Lett.* **2010**, *10*, 4664.
- [130] N. E. Coates, S. Yee, B. McCulloch, K. See, A. Majumdar, R. A. Segalman, J. Urban, *Adv. Mater.* **2013**, *25*, 1629.
- [131] L. Wang, Y. Liu, Z. Zhang, B. Wang, J. Qiu, D. Hui, S. Wang, *Composites, Part B* **2017**, *122*, 145.
- [132] B. T. McGrail, A. Sehirioglu, E. Pentzer, *Angew. Chem., Int. Ed.* **2015**, *54*, 1710.
- [133] M. He, J. Ge, Z. Lin, X. Feng, X. Wang, H. Lu, Y. Yang, F. Qiu, *Energy Environ. Sci.* **2012**, *5*, 8351.
- [134] M. Scheele, N. Oeschler, I. Veremchuk, S.-O. Peters, A. Littig, A. Kornowski, C. Klinke, H. Weller, *ACS Nano* **2011**, *5*, 8541.
- [135] C. Xiao, *Doctoral Degree Thesis*, University of Science and Technology of China, Hefei, China **2016**.
- [136] H. E. Katz, T. O. Poehler, *Innovative Thermoelectric Materials: Polymer, Nanostructure and Composite Thermoelectrics*, World Scientific, Singapore **2016**.
- [137] L. D. Hicks, M. S. Dresselhaus, *Phys. Rev. B* **1993**, *47*, 12727.
- [138] C. Duck-Young, H. Tim, B. Paul, R. L. Melissa, K. Carl, B. Marina, U. Ctirad, M. G. Kanatzidis, *Science* **2000**, *287*, 1024.
- [139] B. Zhang, J. Sun, H. E. Katz, F. Fang, R. L. Opila, *ACS Appl. Mater. Interfaces* **2010**, *2*, 3170.
- [140] Y. Du, K. F. Cai, S. Chen, P. Cizek, T. Lin, *ACS Appl. Mater. Interfaces* **2014**, *6*, 5735.
- [141] K. Wei, T. Stedman, Z.-H. Ge, L. M. Woods, G. S. Nolas, *Appl. Phys. Lett.* **2015**, *107*, 153301.
- [142] H. Ju, J. Kim, *ACS Nano* **2016**, *10*, 5730.
- [143] F. Jiang, J. Xiong, W. Zhou, C. Liu, L. Wang, F. Zhao, H. Liu, J. Xu, *J. Mater. Chem. A* **2016**, *4*, 5265.
- [144] Y. Wang, S. M. Zhang, Y. Deng, *J. Mater. Chem. A* **2016**, *4*, 3554.
- [145] L. Ren, G. Zhang, Y. Zhe, L. Kang, X. Hua, S. Feng, Z. Lei, Z. H. Liu, *ACS Appl. Mater. Interfaces* **2015**, *7*, 28294.
- [146] C. Krishnan, M. Mousumi, K. Kajari, G. Saibal, B. Dipali, *Nanotechnology* **2013**, *24*, 215703.
- [147] A. Arab, Q. Li, *Sci. Rep.* **2015**, *4*, 13706.
- [148] E. W. Zaia, A. Sahu, P. Zhou, M. P. Gordon, J. D. Forster, S. Aloni, Y.-S. Liu, J. Guo, J. J. Urban, *Nano Lett.* **2016**, *16*, 3352.
- [149] Y. Xia, K. Sun, J. Ouyang, *Adv. Mater.* **2012**, *24*, 2436.
- [150] Y. Xia, K. Sun, J. Ouyang, *Energy Environ. Sci.* **2012**, *5*, 5325.
- [151] Y. Chen, M. He, B. Liu, G. C. Bazan, J. Zhou, Z. Liang, *Adv. Mater.* **2017**, *29*, 1604752.
- [152] D. Tasis, N. Tagmatarchis, A. Bianco, M. Prato, *Chem. Rev.* **2006**, *106*, 1105.
- [153] B. Fan, X. Mei, K. Sun, J. Ouyang, *Appl. Phys. Lett.* **2008**, *93*, 143103.
- [154] C. Soldano, A. Mahmood, E. Dujardin, *Carbon* **2010**, *48*, 2127.
- [155] A. D. Avery, B. H. Zhou, J. Lee, E.-S. Lee, E. M. Miller, R. Ihly, D. Wesenberg, K. S. Mistry, S. L. Guillot, B. L. Zink, Y.-H. Kim, J. L. Blackburn, A. J. Ferguson, *Nat. Energy* **2016**, *1*, 16033.
- [156] D. Kim, Y. Kim, K. Choi, J. C. Grunlan, C. Yu, *ACS Nano* **2010**, *4*, 513.
- [157] L. Weber, E. Gmelin, *Appl. Phys. A: Mater. Sci. Process.* **1991**, *53*, 136.
- [158] C. Yu, K. Choi, L. Yin, J. C. Grunlan, *ACS Nano* **2011**, *5*, 7885.
- [159] K. Choi, C. Yu, *PLoS One* **2012**, *7*, e44977.
- [160] G. P. Moriarty, S. De, P. J. King, U. Khan, M. Via, J. A. King, J. N. Coleman, J. C. Grunlan, *J. Polym. Sci., Part B: Polym. Phys.* **2013**, *51*, 119.
- [161] W. Lee, Y. H. Kang, J. Y. Lee, K.-S. Jang, S. Y. Cho, *RSC Adv.* **2016**, *6*, 53339.
- [162] J.-H. Hsu, W. Choi, G. Yang, C. Yu, *Org. Electron.* **2017**, *45*, 182.
- [163] K. Xu, G. Chen, D. Qiu, *J. Mater. Chem. A* **2013**, *1*, 12395.
- [164] L. Liang, C. Gao, G. Chen, C.-Y. Guo, *J. Mater. Chem. C* **2016**, *4*, 526.
- [165] X. Hu, G. Chen, X. Wang, *Compos. Sci. Technol.* **2017**, *144*, 43.
- [166] S. Han, W. Zhai, G. Chen, X. Wang, *RSC Adv.* **2014**, *4*, 29281.
- [167] C. Meng, C. Liu, S. Fan, *Adv. Mater.* **2010**, *22*, 535.
- [168] Q. Yao, L. Chen, W. Zhang, S. Liufu, X. Chen, *ACS Nano* **2010**, *4*, 2445.
- [169] Q. Yao, Q. Wang, L. Wang, L. Chen, *Energy Environ. Sci.* **2014**, *7*, 3801.
- [170] L. Wang, Q. Yao, J. Xiao, K. Zeng, S. Qu, W. Shi, Q. Wang, L. Chen, *Chem. - Asian J.* **2016**, *11*, 1804.
- [171] H. Wang, S.-i. Yi, X. Pu, C. Yu, *ACS Appl. Mater. Interfaces* **2015**, *7*, 9589.
- [172] D. Yoo, J. Kim, J. H. Kim, *Nano Res.* **2014**, *7*, 717.
- [173] J. Xiong, F. Jiang, H. Shi, J. Xu, C. Liu, W. Zhou, Q. Jiang, Z. Zhu, Y. Hu, *ACS Appl. Mater. Interfaces* **2015**, *7*, 14917.
- [174] L. Wang, Q. Yao, H. Bi, F. Huang, Q. Wang, L. Chen, *J. Mater. Chem. A* **2015**, *3*, 7086.
- [175] F. Li, K. Cai, S. Shen, S. Chen, *Synth. Met.* **2014**, *197*, 58.
- [176] Y. Xu, Z. Li, W. Duan, *Small* **2014**, *10*, 2182.
- [177] Y. Zhu, S. Murali, W. Cai, X. Li, J. W. Suk, J. R. Potts, R. S. Ruoff, *Adv. Mater.* **2010**, *22*, 3906.
- [178] M. G. Han, S. H. Foulger, *Small* **2006**, *2*, 1164.
- [179] K. Zhang, S. Wang, J. Qiu, J. L. Blackburn, X. Zhang, A. J. Ferguson, E. M. Miller, B. L. Weeks, *Nano Energy* **2016**, *19*, 128.



- [180] H. J. Lee, G. Anoop, H. J. Lee, C. Kim, J.-W. Park, J. Choi, H. Kim, Y.-J. Kim, E. Lee, S.-G. Lee, Y.-M. Kim, J.-H. Lee, J. Y. Jo, *Energy Environ. Sci.* **2016**, *9*, 2806.
- [181] Q. Wu, J. Hu, *Composites, Part B* **2016**, *107*, 59.
- [182] P. Li, K. Sun, J. Ouyang, *ACS Appl. Mater. Interfaces* **2015**, *7*, 18415.
- [183] P. Li, D. Du, L. Guo, Y. Guo, J. Ouyang, *J. Mater. Chem. C* **2016**, *4*, 6525.
- [184] R. Zhou, P. Li, Z. Fan, D. Du, J. Ouyang, *J. Mater. Chem. C* **2017**, *5*, 1544.
- [185] D. Yoo, J. Kim, S. H. Lee, W. Cho, H. H. Choi, F. S. Kim, J. H. Kim, *J. Mater. Chem. A* **2015**, *3*, 6526.
- [186] J. Choi, J. Y. Lee, S.-S. Lee, C. R. Park, H. Kim, *Adv. Energy Mater.* **2016**, *6*, 1502181.
- [187] E. J. Bae, Y. H. Kang, C. Lee, S. Y. Cho, *J. Mater. Chem. A* **2017**, *5*, 17867.
- [188] C. Cho, B. Stevens, J.-H. Hsu, R. Bureau, D. A. Hagen, O. Regev, C. Yu, J. C. Grunlan, *Adv. Mater.* **2015**, *27*, 2996.
- [189] C. Cho, K. L. Wallace, P. Tzeng, J.-H. Hsu, C. Yu, J. C. Grunlan, *Adv. Energy Mater.* **2016**, *6*, 1502168.
- [190] C. Cho, M. Culebras, K. L. Wallace, Y. Song, K. Holder, J.-H. Hsu, C. Yu, J. C. Grunlan, *Nano Energy* **2016**, *28*, 426.
- [191] M. Culebras, C. Cho, M. Krecker, R. Smith, Y. Song, C. M. Gómez, A. Cantarero, J. C. Grunlan, *ACS Appl. Mater. Interfaces* **2017**, *9*, 6306.
- [192] C. J. An, Y. H. Kang, A. Y. Lee, K.-S. Jang, Y. Jeong, S. Y. Cho, *ACS Appl. Mater. Interfaces* **2016**, *8*, 22142.
- [193] C. Park, D. Yoo, S. Im, S. Kim, W. Cho, J. Ryu, J. H. Kim, *RSC Adv.* **2017**, *7*, 25237.
- [194] C. T. Hong, W. Lee, Y. H. Kang, Y. Yoo, J. Ryu, S. Y. Cho, K.-S. Jang, *J. Mater. Chem. A* **2015**, *3*, 12314.